



Article

The ESA Permanent Facility for Altimetry Calibration: Monitoring Performance of Radar Altimeters for Sentinel-3A, Sentinel-3B and Jason-3 Using Transponder and Sea-Surface Calibrations with FRM Standards

Stelios Mertikas ^{1,*}, Achilleas Tripolitsiotis ², Craig Donlon ³, Constantin Mavrocordatos ³, Pierre Féménias ⁴, Franck Borde ³, Xenophon Frantzis ¹, Costas Kokolakis ², Thierry Guinle ⁵, George Vergos ⁶ , Ilias N. Tziavos ⁶  and Robert Cullen ³

¹ Technical University of Crete, Geodesy and Geomatics Engineering Laboratory, GR 73100 Chania, Greece; xfratzis@mred.tuc.gr

² Space Geomatica P.C., Xanthoudidou 10A, GR 73132 Chania, Greece; admin@spacegeomatica.com (A.T.); c.kokolakis@mred.tuc.gr (C.K.)

³ European Space Agency/European Space Research and Technology Centre (ESA/ESTEC), Keplerlaan 1, AZ 2201 Noordwijk, The Netherlands; craig.donlon@esa.int (C.D.); Constantin.mavrocordatos@esa.int (C.M.); Franck.Borde@esa.int (F.B.); robert.cullen@esa.int (R.C.)

⁴ European Space Agency/European Space Research Institute (ESA/ESRIN), Largo Galileo Galilei, I 00044 Frascati, Italy; Pierre.Femenias@esa.int

⁵ Centre National d'Etudes Spatiales (CNES), CEDEX 31401 Toulouse, France; thierry.guinle@cnes.fr

⁶ Aristotle University of Thessaloniki, School of Geodesy and Surveying, University Box 440, 54124 Thessaloniki, Greece; vergos@topo.auth.gr (G.V.); tziavos@topo.auth.gr (I.N.T.)

* Correspondence: mertikas@mred.tuc.gr; Tel.: +30-28-2103-7629

Received: 6 July 2020; Accepted: 14 August 2020; Published: 16 August 2020



Abstract: This work presents the latest calibration results for the Copernicus Sentinel-3A and -3B and the Jason-3 radar altimeters as determined by the Permanent Facility for Altimetry Calibration (PFAC) in west Crete, Greece. Radar altimeters are used to provide operational measurements for sea surface height, significant wave height and wind speed over oceans. To maintain Fiducial Reference Measurement (FRM) status, the stability and quality of altimetry products need to be continuously monitored throughout the operational phase of each altimeter. External and independent calibration and validation facilities provide an objective assessment of the altimeter's performance by comparing satellite observations with ground-truth and in-situ measurements and infrastructures. Three independent methods are employed in the PFAC: Range calibration using a transponder, sea-surface calibration relying upon sea-surface Cal/Val sites, and crossover analysis. Procedures to determine FRM uncertainties for Cal/Val results have been demonstrated for each calibration. Biases for Sentinel-3A Passes No. 14, 278 and 335, Sentinel-3B Passes No. 14, 71 and 335, as well as for Jason-3 Passes No. 18 and No. 109 are given. Diverse calibration results by various techniques, infrastructure and settings are presented. Finally, upgrades to the PFAC in support of the Copernicus Sentinel-6 'Michael Freilich', due to launch in November 2020, are summarized.

Keywords: satellite altimetry; Copernicus Sentinel-3; calibration; fiducial reference measurements; transponder; sea surface; uncertainty analysis; Crete

1. Introduction

Earth observation is the gathering of information about planet Earth's physical, chemical and biological systems via remote sensing technologies. It is meant to observe our environment, to collect, store and analyze Earth data in order to furnish products for effective decisions on potential risks and vulnerabilities of our planet and its ecosystems.

Satellite altimetry falls in that category of Earth observation. International missions have been measuring geocentric sea level as of 1992 (TOPEX/Poseidon and Jason [1]), with an accuracy, at present, of $\pm 1\text{--}2$ cm. Altimetry measurements coupled with other data from various sea-level observing systems (i.e., tide gauges) have established a long-term record of sea level on global scale. The trend and acceleration of sea level have been found to be $+3.35 \pm 0.40$ mm/yr and 0.12 ± 0.07 mm/yr², respectively, for 1992–2017 [2]. In addition, other acceleration rates of 0.08 ± 0.008 mm/yr² [3] and 0.084 ± 0.025 mm/yr² [4] have been reported.

Sea level rise threatens coasts, and certainly people, through flooding, coastline erosion and submergence, salinization of soil, contamination of underground water, destruction of shoreline defenses, etc. [5–7]. More than 190 million people are at present vulnerable to sea level rise as a result of coastal flooding even under an optimistic scenario of climate change (increase in global warming by 1.0 °C and in sea level by +0.24 m over the period 2046–2065) [8].

Europe, and in particular the European Space Agency (ESA) together with the European Union and Eumetsat, has implemented a large, ambitious and sustained space-based Earth Observation Program, with Copernicus being one of its main components.

Copernicus (<http://www.copernicus.eu/>) is a system for monitoring the Earth in support of European policy. It includes Earth Observation satellites (notably the Sentinel series developed by ESA), ground-based measurements, and services to processes data to provide users with reliable and up-to-date information through a set of Copernicus operational services related to environmental and security issues. These include:

- Copernicus Marine Environmental Monitoring Service (CMEMS (<http://marine.copernicus.eu/>));
- Copernicus Land Monitoring Service (CLMS (<http://land.copernicus.eu/>));
- Copernicus Atmospheric Monitoring Service (CAMS (<https://atmosphere.copernicus.eu/>));
- Copernicus Emergency Management Service (CEMS) (<http://emergency.copernicus.eu/>);
- Copernicus Climate Change Service (C3S) (<http://climate.copernicus.eu/>).

Copernicus services provide critical information to support a wide range of applications, including environment protection, management of urban areas, regional and local planning, agriculture, forestry, fisheries, health, transport, climate change, sustainable development, civil protection and tourism. Copernicus satellite missions are designed to provide 'upstream' inputs to all Copernicus Services as systematic measurements of Earth's oceans, land, ice and atmosphere to monitor and understand large-scale global dynamics.

The primary users of Copernicus services are policymakers and public authorities that need information to develop environmental legislation and policies or to take critical decisions in the event of an emergency, such as a natural disaster or a humanitarian crisis.

The Copernicus programme is coordinated and managed by the European Commission. The development of the observation infrastructure is performed under the aegis of the European Space Agency for the space component and of the European Environment Agency and the Member States for a separate, but important, in-situ measurement component. Copernicus is a programme mandated to make all data products available to subscribing scientists, policy makers, entrepreneurs and the citizens in a full, free, and open access policy.

The space element of Copernicus comprises a family of satellites called "Sentinels", yet exploits data coming from other Earth Observation satellites developed by other agencies. Of particular note are Sentinel-3 and Sentinel-6 that carry a Ku- and C-band radar altimeter and other microwave instruments, designed to observe the topography of the ocean surface, in support of operational oceanography

and monitoring changes in sea level, a key indicator of climate change. These missions also provide information to derive ocean currents, wind speed, ocean heat content and wave height, contributing to maritime safety.

Copernicus has implemented a sustained operational Earth Observation System for the next 20 years with Sentinel satellites, now in place with multiple satellites in each family. For example, Sentinel-3 operates in a sun-synchronous orbit at an altitude of ~800 km, while Sentinel-6 continues the legacy of the TOPEX/Poseidon and Jason series of missions flying at an altitude of ~1300 km at an inclined orbit of 66 degrees—referred to as the ‘altimeter reference orbit’. The Sentinel-6 satellites have been developed by the ESA together with NASA, EUMETSAT, NOAA, and the European Commission with the support of CNES. Still, Jason-3 currently provides operational altimeter measurements following preceding satellite missions occupying the same ground track (including TOPEX/Poseidon, Jason-1 and OSTIM/Jason-2).

A specific set of design and performance requirements is associated with each separate satellite mission to address their primary mission objectives and performance needs. In addition to the Sentinel-3, Sentinel-6 and Jason-3 missions, a number of additional international satellite altimeters either on orbit or shortly to be launched (e.g., CryoSat-2, IceSat-2, SWOT, HY-2C and Quanton), implement diverse measuring technology (interferometry, wide swath and different frequencies), and will contribute to the monitoring of geocentric sea level.

Small differences between successive satellite missions of the same design may be anticipated. If fundamental changes are implemented using new measurement approaches such as synthetic aperture radar (SAR) altimetry, different supporting radiometer channels, or even different choices of microwave radiometer channels, great care must be taken to ensure that such changes do not introduce artificial artefacts into the multi-mission altimetry time series. Furthermore, since range calibration of a satellite altimeter can only be derived effectively once in orbit, a dedicated program of ground-based validation and verification is required.

All satellite altimeters are required to rely upon reference standards and calibration/validation (Cal/Val) infrastructures on the ground to understand relative and absolute differences due to design choices or in-flight degradation of specific components (e.g., antenna, electronics). To maintain an understanding of in-flight performance and maintain the quality of satellite altimetry products, each mission must be regularly monitored using independent data in an objective and absolute sense [9]. This obligation has been implemented using the strategy of Fiducial Reference Measurements (FRM) [9,10] for satellite observations and is supported by the European Space Agency for all its Sentinels.

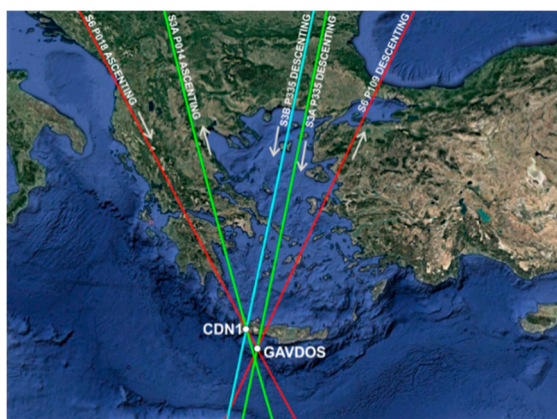
The FRM strategy addresses the need, at first, for Cal/Val facilities to report their results along with a realistic, exhaustive and trustworthy uncertainty budget. It promotes evaluations for the uncertainty of altimetry observations but also to trace uncertainties for water level observations to undisputable standards. It thus aims at achieving reliable, long-term and consistent satellite Earth observations and products, via reliable calibration and standards. It provides a procedure-based service to support the long-term calibration and validation of satellite multi-mission altimetry, and provides independent FRM-class data for use in harmonization of long-term multi-satellite observation of the Earth system, and comprehensive and integrated comparisons and assessments [11].

The Gavdos/Crete facilities in west Crete, Greece have been providing altimetry Cal/Val services since 2004. In 2015, the European Space Agency declared Gavdos facilities as the ESA Permanent Facility for Altimetry Calibration (PFAC) in support of Copernicus altimetry and ESA CryoSat mission calibration and validation activities. Over the past 5 years, the facility has pioneered FRM standards and procedures for altimetry calibration products. The PFAC Cal/Val infrastructure consists of one transponder Cal/Val site for external range calibration that is complemented by three permanent sea-level-surface Cal/Val sites. A second transponder (providing range and sigma-0 retrieval functionality) is being developed for operational redundancy in support of the Copernicus Sentinel-6 mission. The infrastructure that is permanently installed and maintained at the PFAC is

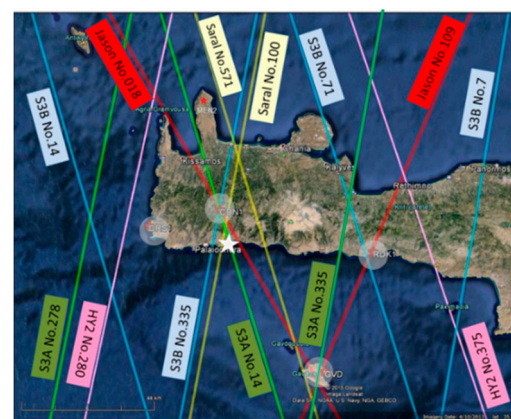
used routinely for multi-mission altimeter calibration activities and additional relative calibration at crossover locations.

The PFAC is designed to allow assessment of different Cal/Val techniques (i.e., sea-surface heights versus transponder) and to perform calibration activities using satellite measurements taken only a few seconds apart along the same orbit. For example, the Sentinel-6 mission will fly 30 s in time apart from Jason-3 along the same nominal ground track for a 12-month tandem flight designed to maintain the stability of the mean sea level trend time series. The ability to perform cross-comparison by diverse and redundant Cal/Val techniques at different settings (at 1050 m, 160 m altitude and at sea level, for example) is required to establish confidence in the calibration results that are derived.

The revisit cycle of Sentinel-3A and -3B is every 27 days and that of Jason-3/Sentinel-6 is every 10 days, with ascending and descending orbits crossing over PFAC Cal/Val transponder infrastructure. This allows the PFAC to support annually about 50 calibrations for each Sentinel-3A and Sentinel-3B satellite and more than 70 calibrations per year for Jason-3 (and subsequently Sentinel-6). It can be seen from Figure 1 that the PFAC calibrates three Sentinel-3A Passes (No. 14, No. 278, and No. 335), three Sentinel-3B Passes (No. 14, No. 71, and No. 335) and two Jason-3 Passes (No. 18 and No. 109).



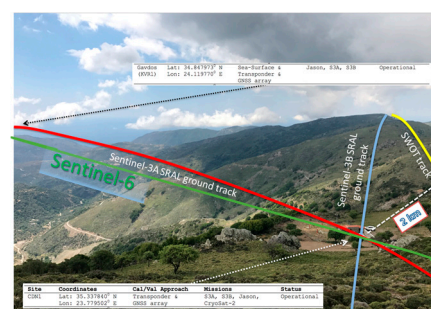
(a)



(b)



(c)



(d)

Figure 1. Cont.

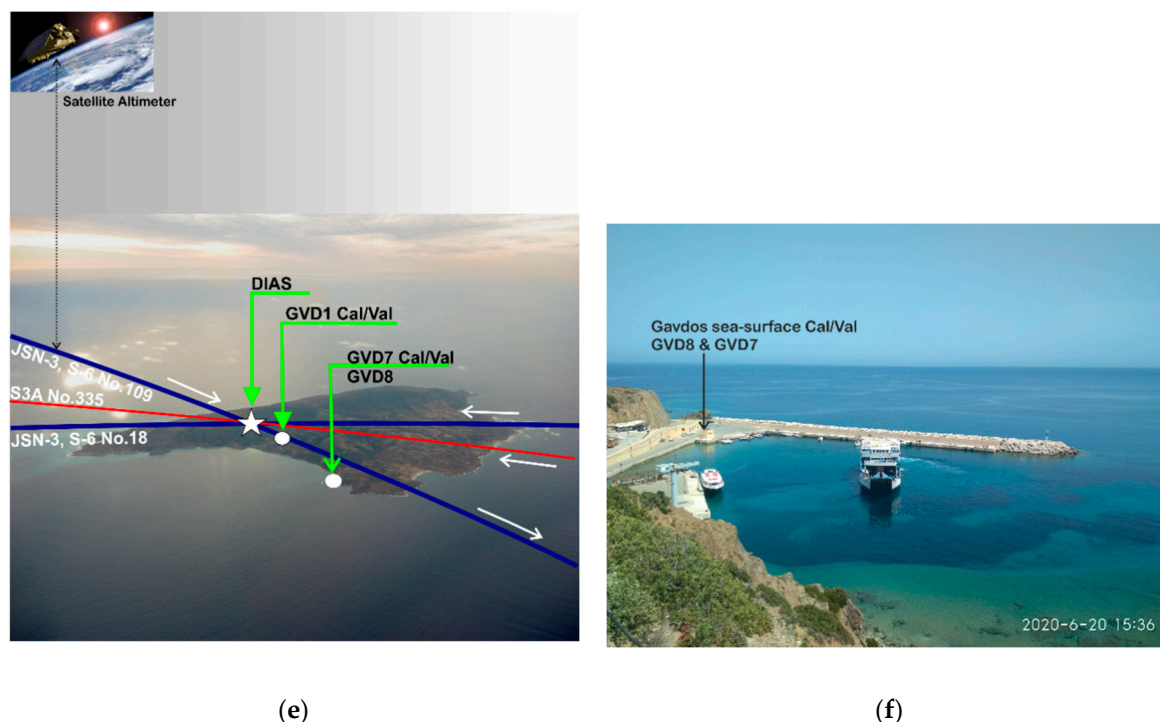


Figure 1. The ground tracks of Sentinel-3A, Sentinel-3B, Jason-3, HY-2B, SARAL/AltiKa over the Permanent Facility for Altimeter Calibration in west Crete, Greece (a). The established Cal/Val sites in Gavdos and Crete (b); the star denotes another coastal tide gauge site of “SUG1” to be established in 2020. The CDN1 transponder Cal/Val on the mountains of mainland Crete (c,d) and the sea-surface Cal/Val sites (GVD7 and GVD8) at the Gavdos harbor (e,f).

This work presents the latest calibration results for Sentinel-3A, Sentinel-3B and Jason-3 as determined at the PFAC, making use of three independent Cal/Val techniques: transponder, sea-surface and crossover analysis. A short description of the PFAC infrastructure and instrumentation is given in Section 2, together with a summary of the three calibration methods employed. The procedures to ensure the Cal/Val measurements (compliant with the FRM standards), and the uncertainty analysis for the sea-surface and transponder calibrations, are described in Section 3. Section 4 presents the absolute Cal/Val results for each satellite (i.e., Sentinel-3A, Sentinel-3B and Jason-3), along with relative calibration results of Sentinel-3A and Sentinel-3B with respect to Jason-3 at crossover locations over the sea surface. Section 5 discusses single-mission results and evaluates performance using each Cal/Val site. Inter-validation of calibration results obtained by diverse Cal/Val methods is also reported. Section 6 summarizes calibration results and the performance of Sentinel-3A, Sentinel-3B and Jason-3 obtained by the PFAC. Finally, future plans for the calibration of the upcoming Sentinel-6 are also discussed.

2. Infrastructure, Instrumentation and Calibration Methods

This section presents the infrastructure and instrumentation of the Permanent Facility for Altimetry Calibration in west Crete, Greece. The principle of operations for each calibration method (i.e., transponder, sea-surface, crossover analysis) employed along with the parametrization of each is also briefly described.

2.1. PFAC Infrastructure and Instrumentation

The location and setting of the Gavdos/Crete Permanent Facility for Altimetry Calibration, in the center of the eastern Mediterranean, offers a unique location for the present generation of multi-mission altimetry calibration (Figure 1).

The PFAC consists of three permanent coastal Cal/Val sites (GVD8 at Gavdos island, CRS1 and RDK1 at the south and west coast of Crete, respectively, Figure 1b) and one transponder Cal/Val site on a mountainous area in the mainland of Crete (Figure 1a). A detailed presentation of these Cal/Val sites has been provided in [12]. Table 1 presents an overview of each Cal/Val site in terms of the altimeters supported, the calibration method employed and its main instrumentation.

Table 1. Summary of existing (PFAC) Cal/Val sites along with the main instrumentation at each Cal/Val site.

Site	Cal/Val Method	Mission/Pass	Instrumentation
CDN1	Transponder	S3A P14 S3B P335 JA3 P18 CryoSat-2	<ul style="list-style-type: none"> • Ku-band range transponder • Microwave radiometer • Two GNSS * receivers • Two meteo stations
GVD8	Sea-Surface	JA3 P18 JA3 P109 S3A P335 S3A P14	<ul style="list-style-type: none"> • Five tide gauges (radar, acoustic, pressure) • Two GNSS receivers • Two meteo stations
RDK1	Sea-Surface	JA3 P109 S3B P71	<ul style="list-style-type: none"> • Two tide gauges (radar) • One GNSS receiver
CRS1	Sea-Surface	S3A P278 S3B P14 HY-2B P280	<ul style="list-style-type: none"> • Two tide gauges (radar, pressure) • One GNSS receiver • One meteo station

* Global Navigation Satellite System.

These instruments are accessed and controlled remotely. Their field observations are transmitted to, via satellite and/or GPRS communications link, and directly archived at the PFAC Operations Control Center at the Technical University of Crete, Greece. Details of the data processing techniques and analysis of raw measurements are given in Section 3.

Two more calibration sites are currently under development: A sea-surface-elevation Cal/Val site at the south coast of Crete (SUG1, Figure 1) and a second transponder Cal/Val site (GVD1) on Gavdos island to support Sentinel-6 Cal/Val activities. A summary of the new GVD1 site is provided in Section 6.

2.2. Calibration and Validation Methods

Independent calibration and validation activities are required to assess the end-to-end performance characteristics of satellite altimeter measurements. Cal/Val activities monitor the measurement uncertainty, stability and behavior, providing independent knowledge of measurement quality. External techniques that regularly support post-launch calibration of satellite altimeters include: (1) sea-surface Cal/Val, (2) transponder Cal/Val, (3) backscatter coefficient Cal/Val, (4) crossover analysis, (5) tandem phase analysis, and (6) comparison to tide gauge networks. The latter is an indirect method, which compares the altimeter-derived sea surface heights with measurements obtained by a global network of tide gauges [13]. Details on PFAC-employed Cal/Val techniques can be found in [14]. A short description of the remaining four techniques and their implementation in the PFAC is given in the following sections.

2.2.1. Sea-Surface Cal/Val

Satellite altimeters are designed to measure the sea (or water) surface height (SSH) above a reference ellipsoid. The sea-surface calibration method compares the sea surface height, as measured by a satellite

altimeter at a certain location and time in open water, to sea surface heights measured by reference ground measurements. A number of corrections need to be applied to the measured satellite range to account for propagation errors caused by the atmosphere (ionosphere, wet and dry troposphere), the sea state bias due to surface roughness impacting the radar measurement, and geophysical corrections including solid earth tide, ocean tides, etc. Ideally, the bias of an altimeter-derived sea-surface height is determined as the difference between the satellite and the ground-truth observations implemented at the same location and time.

Ground-truth observations are provided by a combination of water level sensors, absolute positioning receivers, meteorological and oceanographic sensors, and models of the geoid, tides, mean dynamic topography, etc. At the PFAC, the land mass of Gavdos and Crete contaminates the altimeter's signal, leading to invalid sea-surface measurements close to the coast (about 7.5 km). To overcome this, the Cal/Val site observations have to be transferred to the open sea at about 20 km, with about 3000 m depth, far from the coast where valid satellite measurements exist. This introduces an uncertainty in the approach compared to the ideal case where truly contemporaneous and co-located measurements are available.

2.2.2. Transponder Cal/Val

The sea-surface calibration method compares a derived geophysical parameter (sea-surface height or sea-surface anomaly) at a close-by location with ocean truth measurements regularly made on the coast. Nonetheless, the primary measurement of radar altimeter is the propagation time (converted to range if multiplied by speed of light) of a signal pulse from the altimeter antenna to the Earth's surface and back to the satellite. A transponder provides absolute calibration of these direct and fundamental range observations made by the altimeter if the location of the transponder and its internal path delay are precisely and accurately known.

An active microwave transponder receives the altimeter's signal when a satellite flies over it (which takes about 4 s), amplifies it with minimum distortion and sends it back to the satellite where it is recorded. At first, the received signal is distinctly separated from other surrounding reflections (clutter) of the ground surface as it had been powerfully amplified by the transponder. Then, at explicitly the same time, the geocentric positions of the altimeter in orbit and the transponder on the ground are determined. The theoretical distance between these two instruments in space is subsequently computed. Finally, after extensive processing, the observed range by the altimeter is compared against the theoretical range of the transmitting satellite point in orbit and the center of the transponder. During the overpass period, a time series of the differences between the observed range and the theoretical range provides an estimate of the altimeter range, if short time scale atmospheric components of the troposphere are sufficiently known.

The PFAC has been providing transponder calibration services for Jason-2, Jason-3, CryoSat-2, Sentinel-3A, and Sentinel-3B from September 2015 as part of the ESA FRM4ALT project. After each calibration, the echo of the transponder response is recorded by the altimeter and two recent such examples are shown in Figure 2. Transponder calibrations presuppose that the Agency operating the satellite has programmed the altimeter to observe within the measuring window of the CDN1 Cal/Val site on the mountains at the elevation of 1050 m.

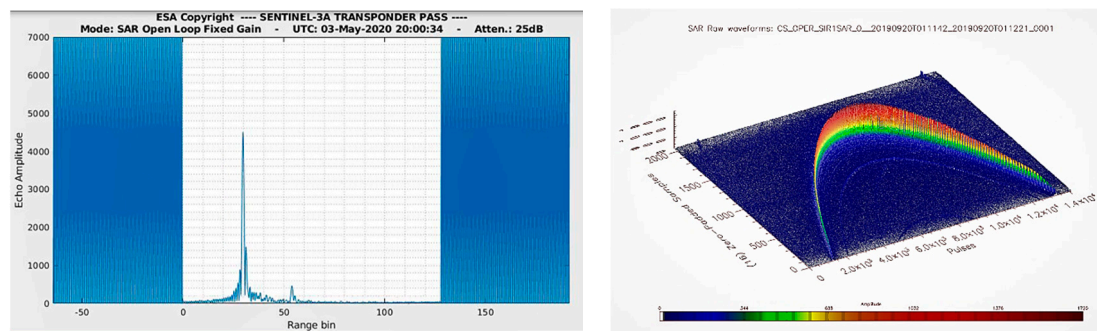


Figure 2. Transponder responses as captured by Sentinel-3A (left) and CryoSat-2 (right, Credit: ESA), Marco Fornari) altimeters during the transponder calibrations carried out on 3-May-2020 and 20-Sept-2019, respectively.

2.2.3. Backscatter Coefficient Cal/Val

In addition to the signal propagation time, a radar altimeter measures the power level of these radar signals [15]. The relation between the amplitude of the transmitted and received echo signals provides information about the characteristics of the imaged surface on the ground. This is expressed as the back-scatter coefficient (sigma-naught, or sigma-0). The sigma0 coefficient is used to retrieve wind speed, and empirical models for the sea state bias required to determine sea surface height.

Calibration of the sigma-naught coefficient can be obtained using either active or passive targets with known and stable radar cross-section, as they are easily detected within the altimeter backscatter records. Previously, a sigma-naught transponder was developed by the European Space Agency and used to calibrate the ENVISAT RA-2 altimeter [16]. This old transponder has been recently (2019) refurbished and is expected to support Sentinel-3 sigma-naught calibrations in 2020 [17].

In support of Copernicus Sentinel-6, a new range and sigma-naught transponder is currently under development and is expected to be installed at the PFAC. The new processing technique of fully focused SAR altimetry [18] may also provide sigma-naught calibration with passive corner reflectors [17] and this will also be investigated at the PFAC. Details on these future plans are given in Section 6.

2.2.4. Crossover Analysis

This technique aims at providing relative calibration between two or more contemporaneous satellite altimeters [19]. The analysis usually takes place on a global scale and at locations where the ascending and descending ground-tracks of altimeters intersect. A crossing event occurs when the time difference of the intersecting passes of two (or more) missions is commonly less than two days [20]. Under the tenuous assumption that the variability and signature of sea level has not changed significantly in the two-day lag between measurements, the sea surface height at the crossover location, as determined by the two missions, can be compared. A significant advantage of this relative performance approach is that it does not require ground measurements and can be performed throughout the missions' lifetime and on a global scale [19].

At the PFAC, the crossover analysis has been modified and applied to retrieve the relative bias of Sentinel-3A Pass No. 14 and Jason-3 Pass No. 109 about 20 km south of Gavdos (Figure 3).

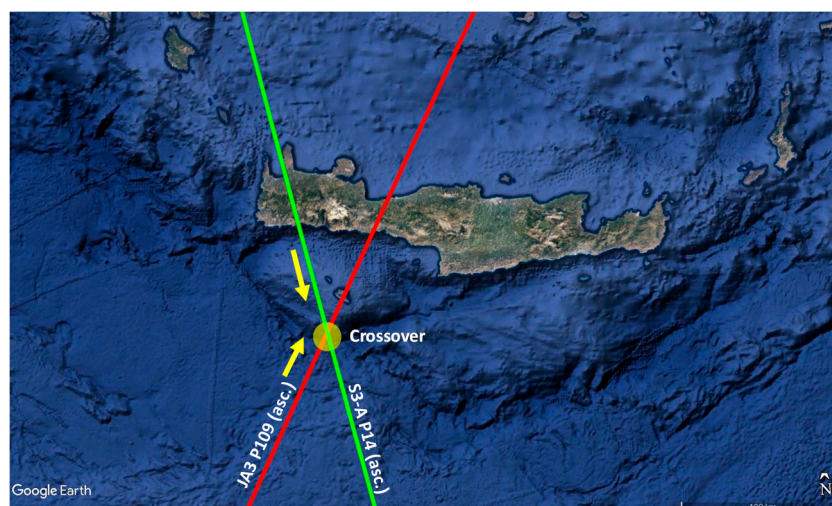


Figure 3. An intersection of the Sentinel-3A Pass No. 14 and Jason Pass No. 109 occurs about 20 km south of Gavdos, Crete, Greece. This location is used to perform crossover analysis and determine the relative bias between the two altimeters.

2.2.5. Tandem Phase Cal/Val

The ideal scenario to characterize the relative bias between two altimeters is to make them observe the same location of the Earth at the same time or a few seconds apart [21]. This is accomplished during a tandem phase, which many new satellite missions incorporate into their regular operations. During this phase, the newly launched satellite is placed on the same orbital track as a reference orbit. The two satellites fly in unison on the same orbit but separated only some seconds apart. For example, Sentinel-3B flew in tandem [22] with Sentinel-3A for four months (6-June-2018 to 16-October-2018) before being placed on its nominal orbit. Similarly, Jason-3 was flying in tandem with Jason-2 with a temporal distance of 80 s for six months (12-February-2016 to 2-October-2016). In [12], the PFAC-derived calibration results of the Jason-2/Jason-3 tandem phase have been presented. The present plan for the future Sentinel-6 will implement a 12-month tandem phase with Jason-3, where the two satellites will fly 30 s apart [23].

This work (see Section 4) presents the relative calibration results from the Sentinel-3 A/B tandem phase. The following Section presents the PFAC's in-situ measurements, the models employed, and the processing strategies followed for the implementation of the aforementioned calibration methodologies for Sentinel-3A, Sentinel-3B and Jason-3 altimeters for absolute and relative calibration.

3. The PFAC Measurements and the FRM Uncertainty Analysis

In-situ measurements used for external calibration and validation of Earth observation have to follow and be traceable to internationally agreed reference standards. In addition, the uncertainty analysis of these measurements has to accompany the respective Cal/Val results. This uncertainty should be available to allow altimetry operators to evaluate the credibility and suitability of the Cal/Val results for efficient monitoring of the altimeter's performance. A strategy for assuring a uniform and absolute standardization for calibrating satellite altimeters is given in [24]. The main uncertainty constituents for sea-surface and transponder Cal/Val techniques have been identified in [9] and quantified in [14].

Accurate determination of the absolute geodetic coordinates for a Cal/Val site constitutes one of the key uncertainty components in both sea-surface and transponder calibration. Particularly, the height component is of utmost importance as it controls both the sea-surface height at the sea-surface Cal/Val site and the distance between the transponder and altimeter phase center. The following section presents the strategy followed at the PFAC to determine the absolute coordinates of the Cal/Val sites

and their uncertainty. Later, the remaining constituents of uncertainty contributing to each calibration method are examined separately.

3.1. Absolute Coordinates Constituent

In the PFAC, a network of continuously operating GNSS stations distributed in western Crete and Gavdos (Figure 4) provides absolute geodetic coordinates and velocities for reference points at each Cal/Val site.

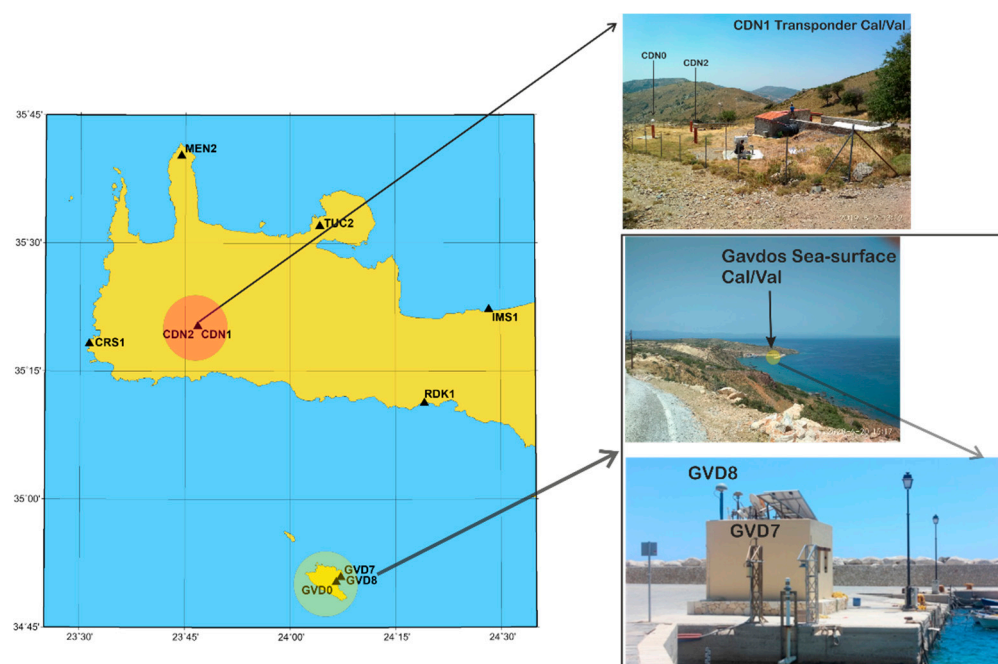


Figure 4. Location of the geodetic GNSS network that provides absolute coordinates of the PFAC Cal/Val sites (left, map of west Crete). Example photos from the main sea-surface Cal/Val facility in Gavdos and the CDN1 transponder Cal/Val site on the mountains of Crete. Operations of two GNSS receivers at each Cal/Val site ensures redundancy and reliability of observations.

According to FRM requirements, redundancy of the scientific equipment has to be ensured. This implies that at least two instruments should operate side by side to measure the same parameter to ensure that any potential errors and drifts in the operations are identified. For example, Table 2 presents the coordinates and velocities for the two GNSS receivers operating at the CDN1 transponder Cal/Val site (CDN0 and CDN2) and the two operating at the Gavdos sea-surface facility (GVD7 and GVD8). All sites have been processed using the GAMIT scientific software, which applies relative positioning techniques [25]. The reference epoch of these coordinates and velocities is 2013.5 and the geodetic frame used is the ITRF 2014.

In order to assess the values for the ellipsoidal height for each pair of the GNSS receivers (i.e., the CDN0 with the CDN2 and the GVD7 with the GVD8) their antenna reference points have to be geodetically tied together but also connected to other reference control points in the vicinity. This task is achieved through precise leveling that provides height differences with uncertainty of the order of ± 1 mm. These levelling surveys are carried out on a semi-annual basis as well as during a major event (i.e., GNSS antenna replacement, earthquake, etc.). The derived uncertainty of GNSS processing is given in Table 2. The final value for uncertainties in the determination of absolute coordinates for the reference benchmarks on each Cal/Val site are used as input in the processing chain to derive the FRM constituent uncertainty.

Table 2. The International Terrestrial Reference Frame 2014 (ITRF2014) coordinates and velocities of two pairs of GNSS stations operating at the CDN1 transponder (CDN0 and CDN2) and Gavdos sea-surface (GVD7 and GVD8) Cal/Val sites. The time span and uncertainties in the form of a weighted root mean square error of each component are also given.

Site/Time Span	Lat [degree]	Lon [degree]	Ellipsoid Height [m]	N_velocity [m yr ⁻¹]	E_velocity [m yr ⁻¹]	UP_velocity [m yr ⁻¹]
CDN0 [2014.49–2019.99]	N35°20′16.024375″ ±3.1 mm	E23°46′46.854809″ ±2.1 mm	1049.5186 ±8.0 mm	−0.0126 ±0.3 mm	0.0076 ±0.5 mm	0.0002 ±1.0 mm
CDN2 [2016.40–2019.99]	N35°20′16.291109″ ±1.8 mm	E23°46′46.829112″ ±2.2 mm	1050.4068 ±8.5 mm	−0.0127 ±0.4 mm	0.0070 ±0.5 mm	−0.0025 ±2.0 mm
GVD7 [2009.37–2019.55]	N34°50′52.744568″ ±1.6 mm	E24°7′11.205643″ ±2.2 mm	20.1685 ±6.0 mm	−0.0137 ±0.1 mm	0.0083 ±0.2 mm	−0.0004 ±0.5 mm
GVD8 [2010.36–2019.99]	N34°50′52.612211″ ±1.8 mm	E24°7′11.399214″ ±2.2 mm	22.2760 ±6.4 mm	−0.0143 ±0.2 mm	0.0078 ±0.2 mm	0.0004 ±0.5 mm

GNSS Processing Constituent

The positioning results presented in Table 2 are those derived by relative positioning processing. Using the same GNSS observations, the alternative technique of Precise Point Positioning (i.e., GIPSY scientific software [26]) is also applied to derive solutions for the coordinates and velocities of the same GNSS stations. Processing of the same GNSS observations with different processing strategies ensures validity of the derived absolute positioning values, and follows the FRM4ALT study recommendation to use multiple approaches to arrive at the same result [24]. The results of different processing strategies are shown in Figure 5 for the GVD8 Cal/Val site in Gavdos.

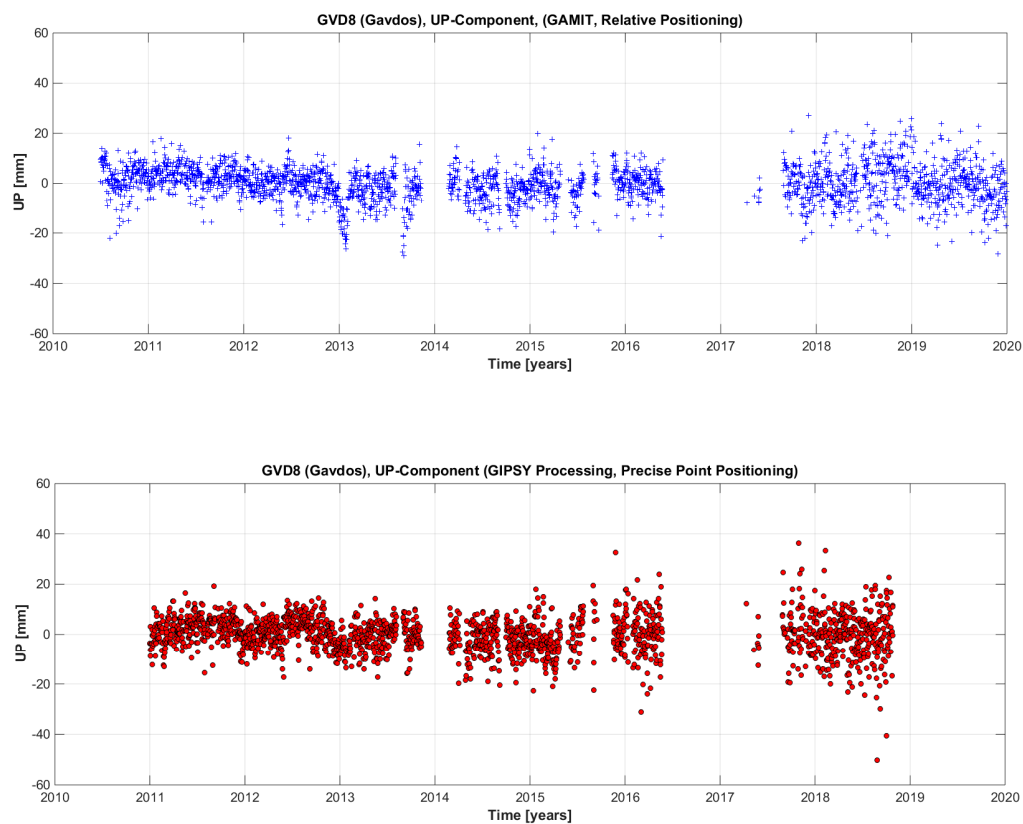


Figure 5. Dispersion values for the height component of the GVD8 GNSS station in the form of coordinate time series as derived by relative differential (upper image) and precise point positioning processing (lower image). The reference epoch is 2013.5 and solutions refer to the ITRF2014 reference frame. The gap observed in the period between 2016.5 and 2017.6 corresponds to construction works carried out at the Gavdos harbor that forced temporary decommissioning of GVD8.

The coordinates and velocities of each GNSS station as determined by diverse GNSS processing techniques have been found to agree at the mm-level and sub-mm level, respectively (Table 3).

Table 3. GNSS processing results (Cartesian coordinates and velocities) for the GVD8 station as derived by the relative differential and precise point positioning techniques.

GVD8 Station	Relative Differential	Precise Point Positioning	Difference
X [m]	4,782,603.4086	4,782,603.4080	0.6 mm
Y [m]	2,141,348.9747	2,141,348.9748	0.1 mm
Z [m]	3,624,048.9145	3,624,048.9142	0.3 mm
V_X [m/yr]	0.0042	0.0035	0.7 mm/yr
V_Y [m/yr]	0.0105	0.0104	0.1 mm/yr
V_Z [m/yr]	−0.0117	−0.0117	0.0 mm/yr
Time Span [yr]	2010.4973–2019.1712	2011.0060–2019.1743	

In the following subsection, the uncertainty for the sea-surface and transponder Cal/Val, as implemented at the PFAC, is given along with the verification that in-situ measurements are in compliance with the FRM4ALT standards.

3.2. Uncertainty Budget for Sea-Surface Calibration

Apart from the uncertainty constituent in the determination of the absolute coordinates for the Cal/Val site, presented in Section 3.1, other major contributing sources of uncertainty in sea-surface calibration are: (1) determination of the sea-surface height at the Cal/Val location, (2) transfer of sea-surface height from the Cal/Val site to open sea, and (3) processing errors. Estimations of the uncertainties at the PFAC are explained using indicative examples.

3.2.1. Sea-Surface Height Constituent

Measurements obtained by tide gauges are used to determine the sea surface height above a reference ellipsoid at the PFAC Cal/Val sites. According to FRM standards, at least two such instruments of diverse make and operating principle are to operate at each site. This redundant instrumentation permits efficient monitoring of each instrument's performance and inter-validation of their measurements. For example, in Gavdos Cal/Val, there are five continuously operating tide gauges: KVR3 (radar), KVR4 (acoustic), KVR5 (pressure), KVR6 (radar and operating in a stilling well) and KVR7 (radar) (Figure 6).

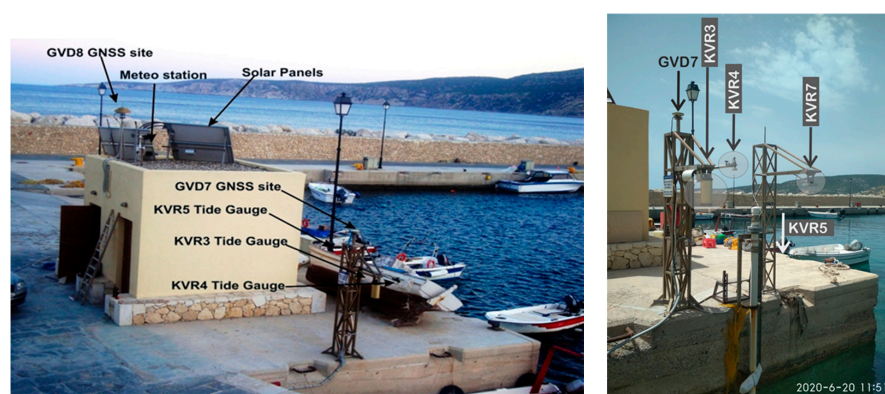


Figure 6. The current set up of the “Karave” Cal/Val site in Gavdos harbor for sea-surface calibrations. Five tide gauges (KVR3-radar, KVR4-acoustic, KVR5-pressure, KVR6-radar in a stilling well, and KVR7-radar), two GNSS receivers (GVD7 and GVD8) and one meteorological station comprise the main scientific instrumentation of the Gavdos Cal/Val site.

The overall performance of these tide gauges is monitored on a daily and/or monthly basis. A 24-h recording of four of those tide gauges, on 14-Oct-2019, is given in Figure 7.

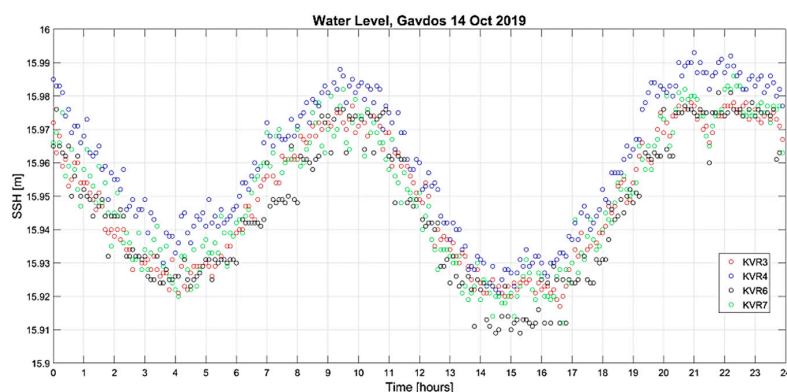


Figure 7. Single-day (14-October-2019) water level measurements of the KVR3 (radar), KVR4 (acoustic), KVR6 (radar in a stilling well) and KVR7 (radar) tide gauges operating at the Gavdos Cal/Val site.

A more detailed analysis of water level observations involves, among others, the evaluation of the Van de Castele diagrams on a daily basis. The shape of the Van de Castele diagram provides a qualitative illustration of the type of error involved in tide gauge measurements [27]. Simultaneous water level heights of a certain tide gauge are compared against a master reference tide gauge (Figure 8). The x-axis corresponds to the difference between the two tide gauge measurements over a full tidal cycle. The y-axis is the “true” sea-surface height as measured by the reference tide gauge. The shape of the diagram may be used to identify the source of any deviation between the measurements obtained by the reference and the tide gauge under investigation [28].

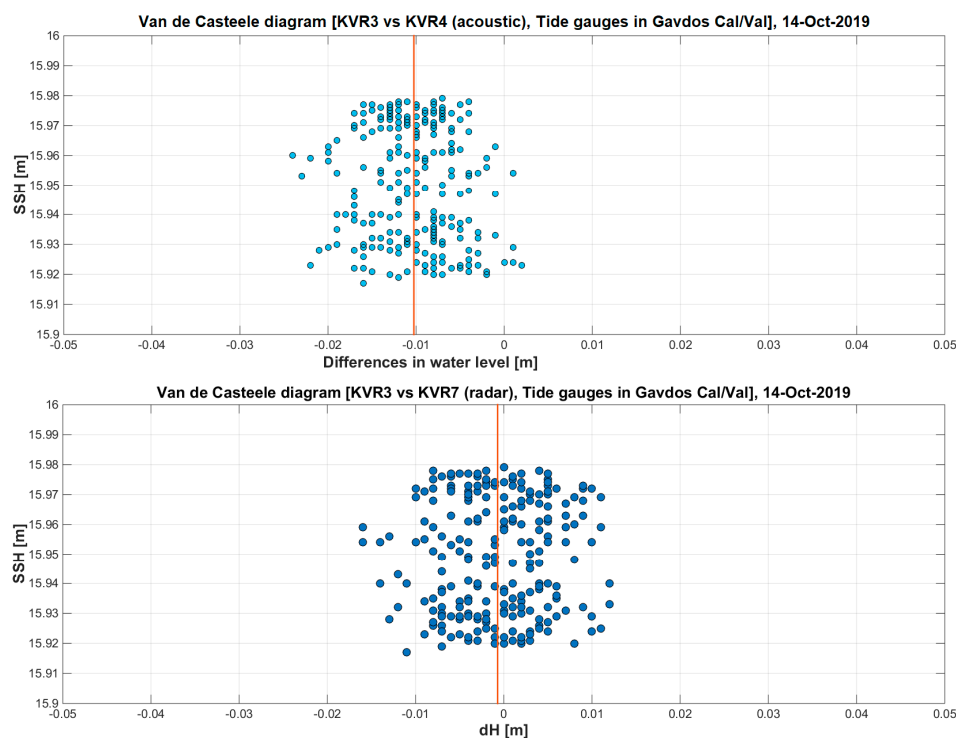


Figure 8. The Van de Castele diagrams applied for tide gauge records at the Gavdos Cal/Val site on 14 October 2019. The radar KVR3 sensor is considered to be the reference against which the performance of the acoustic KVR4 (upper), and radar KVR7 (lower) tide gauges is evaluated. Each diagram represents the sea level (SSH, y axis) versus the difference between records of the two instruments (ΔH , x-axis). The sampling rate is 6min.

In Gavdos, the KVR3 radar tide gauge is considered to be the reference water level sensor. The Van de Casteele test is applied and the performance of the remaining tide gauges (i.e., KVR4, KVR6, KVR7) is monitored. Various sampling intervals exist for the different tide gauges. In order to apply the Van de Casteele diagram, the daily tide gauge records are averaged, when needed, to match a 6-min sampling interval. Figure 8 presents an indicative example of such a single day (14-October-2019) monitoring for the KVR4 and the KVR7 sensors. It can be seen that, for this particular day, all tide gauge records agree with an uncertainty of the order of ± 1 cm.

Monitoring of the long-term performance of all tide gauges with an external and independent system without interrupting their measurements poses a challenge in the PFAC operations. Two approaches are followed: In the first, the monthly means of each tide gauge measurement are monitored to verify their overall performance. The second uses an external reference instrument (i.e., tide pole) for sea-surface height determination. A leveling survey is carried out to tie the tide pole and tide gauge reference points. The Van de Casteele diagrams are again created, but using the tide pole as reference. This procedure is carried out at least once per year and a detailed record is kept. If the difference between the tide pole and one of the tide gauges exceeds certain criteria (i.e., 1 cm), then the external validation is repeated within two months. If the difference continues to exceed the criteria set, then the tide gauge is decommissioned and sent to external facilities for calibration. This technique is also used to precisely estimate the electrical center, i.e., the measuring reference point (“zero” point) of the tide gauge records.

3.2.2. Reference Surface Constituent

In the PFAC, the sea-surface height has to be transferred from the Cal/Val location in the harbor to open sea where satellite measurements are made uncontaminated by land mass (about 20 km away). To accomplish this transfer, the reference geoid and the mean dynamic topography (MDT) have to be accurately known. In the past, terrestrial, marine and airborne gravity surveys have been carried out in the vicinity of the PFAC Cal/Val sites. Regional geoid and MDT models have been developed and validated by dedicated field campaigns using boats and buoys. Details on those reference surfaces are presented in [29].

In 2018, additional gravity field measurements have been carried out at the PFAC Cal/Val sites and around the Gavdos island (Figure 9). A CG-5 microgravity sensor with a resolution of 1 μ Gal and standard deviation less than 5 μ Gals has been used. Three control points with known absolute gravity values have been chosen as reference points to conduct this gravity survey. Absolute gravity measurements have been conducted in the past by the Hellenic Military Geographical Service and international research institutes. These absolute gravity points are located at Chania Airport (AIR), and Sfakia (SFK) and Paleochora (PAL) villages (Figure 9). Absolute gravity values for various locations at the PFAC sites have been determined by relying upon those absolute reference points (AIR, PAL, SFK), and measuring relative gravity between them and the PFAC Cal/Val sites. These new gravity observations have been incorporated in the regional gravity database to improve the geoid accuracy.



Figure 9. Terrestrial gravity measurements carried out in 2018 at various locations around the PFAC Cal/Val sites in Crete (top-left) and Gavdos (top-right). Locations with known absolute gravity values are marked with a triangle. Gravity observations are shown at the PAL absolute gravity point in south Crete (bottom-left), the RDK1 (bottom-middle) and Karave/Gavdos (bottom-right) Cal/Val sites.

3.2.3. FRM Uncertainty Estimation for Sea-Surface Calibration

For sea-surface calibration, the principal sources of uncertainty arise from (1) absolute coordinates of the Cal/Val site (Section 3.1), (2) the sea-surface heights (Section 3.2.1), and (3) the reference surfaces to transfer sea-surface heights to open sea (Section 3.2.2). A complete list and analysis of various constituents of uncertainty involved in sea-surface calibration may be found in [10]. The uncertainty for each constituent is classified into two categories: Type A and Type B. Their leading difference is that Type A uncertainties are evaluated by statistical analysis of observations, whereas Type B ones are estimated by scientific judgment based on manufacturer's specs, prior experience, handbooks, etc. [30].

Table 4 quantifies the uncertainty for the sea-surface Cal/Val as implemented in the PFAC. It also updates the uncertainty budget analysis that has been previously presented in [14,24]. The FRM standardized uncertainty at a 68% confidence level for the sea-surface calibration is calculated to be ± 31.91 mm.

Table 4. Uncertainty budget for the sea-surface calibration. The final standardized uncertainty (at 68% confidence level), described by a Root-Sum-Square value, has been computed as:

$$FRM_{SSH}(Uncertainty) = \pm 31.91 \text{ mm} = \sqrt{(0.10)^2 + (3.50)^2 + (2.00)^2 + \dots + (0.30)^2 + (5.80)^2 + (11.55)^2}.$$

Error Constituent	Type	Uncertainty Estimate	Standard Uncertainty (Confidence 68%)
GNSS Height Repeatability ¹	A	0.10 mm	±0.10 mm
GNSS Receiver ²	B	6.00 mm	±3.50 mm
GNSS Antenna Reference Point ¹	B	2.00 mm	±2.00 mm
Water Level ¹	B	1.30 mm	±1.30 mm
Tide-Gauge Zero Reference ¹	A	0.15 mm	±0.15 mm
Tide Gauge Vertical Alignment ²	B	2.40 mm	±1.39 mm
Tide-Gauge Sensor Certificate ¹	B	5.50 mm	±5.50 mm
Leveling Repeatability ¹	A	0.11 mm	±0.11 mm
Monumentation ²	B	1.10 mm	±0.64 mm
Vertical Misalignment ²	B	1.00 mm	±0.60 mm
Leveling Observer ²	B	1.00 mm	±0.60 mm
Leveling Instrument/Method ²	B	1.00 mm	±0.60 mm
Tide Pole Reading During Calibration ²	B	1.00 mm	±0.60 mm
Geoid and Mean Dynamic Topography ¹	B	30.00 mm	±30.00 mm
Processing and Approximations ²	B	0.50 mm	±0.30 mm
Geoid Slope/Offshore Transfer ²	B	10.00 mm	±5.80 mm
Unaccounted effects ²	B	20.00 mm	±11.55 mm
Root-Sum-Squared Uncertainty			±31.91 mm

¹ assuming that residuals are random and normally distributed, with no autocorrelation. ² assuming that uncertainty constituents follow the uniform distribution.

3.3. Uncertainty Budget for Transponder Calibration

Following a similar analysis, the FRM uncertainty for the transponder calibration has also been determined. Here, the atmospheric propagation delays of satellite signals and the transponder's internal delay dominate the overall uncertainty [9].

3.3.1. Atmospheric Propagation Delay Constituent

Determination of the signal delays caused by the atmosphere constitutes the most challenging task in transponder calibration. This is because the radiometer on-board the satellite does not operate properly over land. Thus, other means have to be figured out to correct signal propagation delays when the altimeter flies over a transponder land site. In the PFAC, this is carried out using GNSS-derived corrections for the atmospheric delays.

The GNSS-derived delays refer to both the ionospheric and the zenith tropospheric (wet and dry component) delays at the transponder Cal/Val site. The ionosphere delays over the PFAC are regularly stable. They do not change rapidly and can be accurately determined via GNSS processing with an uncertainty of the order of ±1 mm [24]. The dry (or hydrostatic) troposphere delay is also stable. It can also be accurately modeled using in-situ surface pressure measurements made by meteorological sensors. The wet component of the troposphere is dynamic, presents unstable variability rapidly changing over time, and cannot be easily modeled. In GNSS processing, this wet troposphere delay is estimated as the remaining part of the total delay minus the dry troposphere delay. Different GNSS processing methodologies generate diverse atmospheric propagation delays (Figure 10).

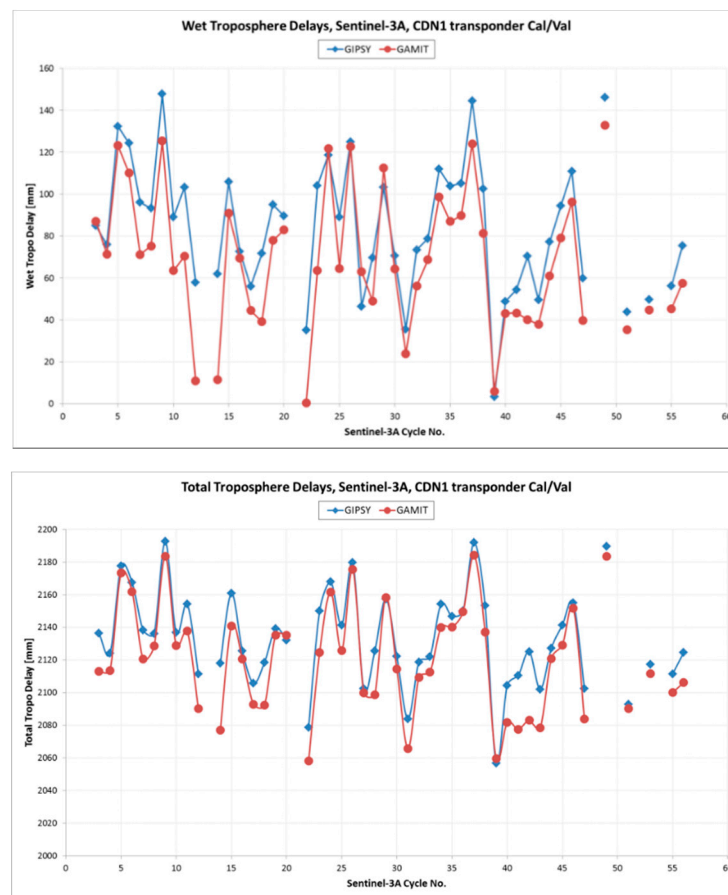


Figure 10. The wet troposphere (up) and total troposphere (down) delays coming out after GNSS processing with precise point positioning (GIPSY) and relative differential (GAMIT) positioning during Sentinel-3A Pass No. 14 transponder calibrations at the CDN1 Cal/Val site.

The difference observed in Figure 10 may be attributed to various models applied to determine the dry troposphere delay in their derivation, the means implemented to estimate surface pressure (i.e., models or in-situ measurements), as well as to the sampling rate used for GNSS data processing (Figure 11).

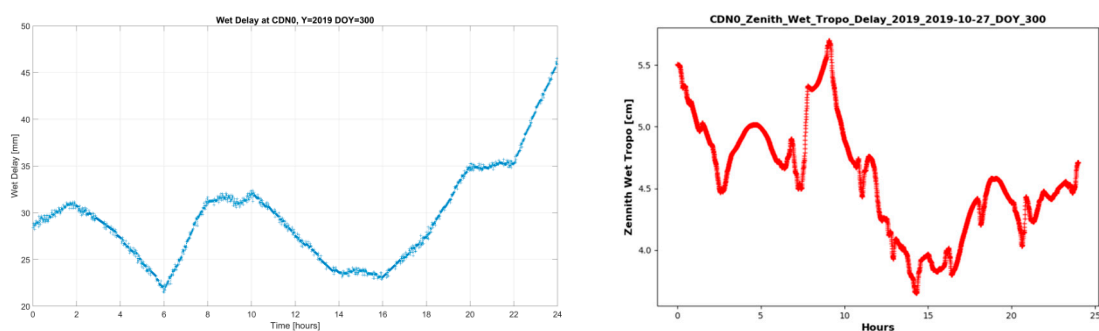


Figure 11. Hourly zenith wet delays as estimated by GNSS processing using relative differential positioning (left) and precise point positioning (right) for the Sentinel-3A transponder calibration, on 27-October-2019 at the CDN1 transponder Cal/Val site.

In order to be FRM-compliant, the PFAC should verify the GNSS-derived wet tropospheric delays at the time of satellite overpass using an independent technique. A ground microwave radiometer, provided on loan from the European Space Agency, has been installed in 2019 at the CDN1

transponder Cal/Val site to fulfill this FRM requirement (Figure 12). This instrument measures the brightness temperature of microwave radiation from the atmosphere and determines the respective contribution/attenuation from water vapor and liquid water. Preliminary results indicate an agreement of the wet troposphere delays from the radiometer and the GNSS-derived delays. At this preliminary stage, dispersion of wet delay is in the order of $\pm 1\text{--}2$ cm (maximum) (Figure 12). Research and field measurements are ongoing. As more data are built up, more robust and reliable results on the final wet troposphere estimation will be estimated.

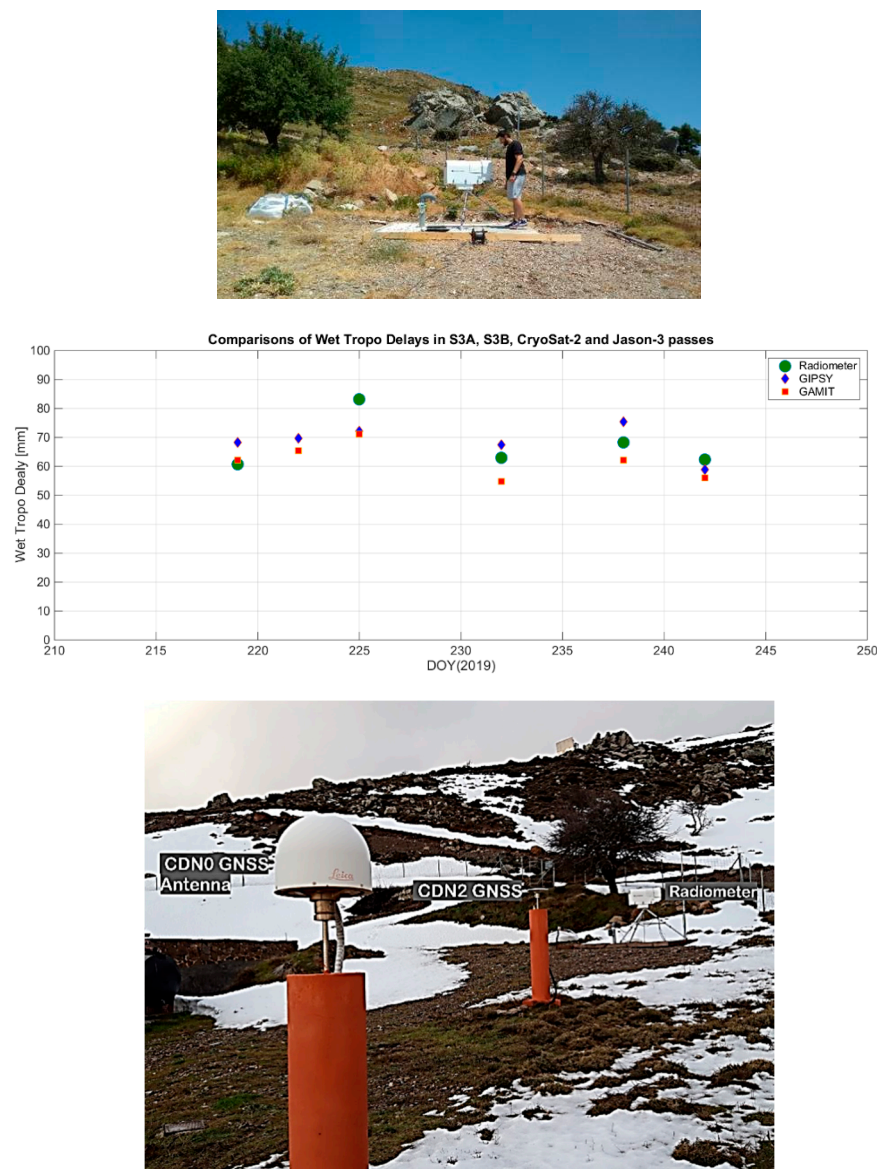


Figure 12. The microwave radiometer operating at the CDN1 transponder Cal/Val site (upper image) and preliminary assessment of GNSS-derived wet tropospheric delays against radiometer's measurements (middle). The lower picture shows the setup of the radiometer and the two GNSS stations.

An alternative technique to determine wet tropospheric delay can be derived from measurements of the imaging spectrometer flown aboard the Sentinel-3 mission. It relies upon the Integrated Water

Vapor (*IWV*) products derived from the Ocean and Land Color Instrument (OLCI). There is a direct relation between the zenith wet delay (*ZWD*) and the *IWV*, Equation (1).

$$IWV_{OLCI} = [F] \cdot ZWD = \left[\frac{10^6}{\rho \cdot R_V \cdot \left(\frac{C_1}{T_m} + C_2 \right)} \right] \cdot ZWD \quad (1)$$

where: *F* is a temperature-dependent factor given in the right-hand equation, *IWV* is the atmospheric water vapor content in (kg m^{-2}), ρ is the mass density of water, R_V the gas constant for water vapor in ($\text{N M K}^{-1} \text{ gr}^{-1}$), C_1 and C_2 are refractivity coefficients in ($\text{K}^2 \text{ hPa}^{-1}$) and (K hPa^{-1}), respectively, T_m is the weighted temperature of the atmosphere in ($^\circ\text{K}$) and *ZWD* is the zenith wet delay caused by the wet troposphere in (mm).

The OLCI instrument of Sentinel-3 has a swath of 1270 km and thus permits global coverage within 2 days. OLCI is an optical instrument that captures images during daytime. The spatial resolution of these images is 300 m (at nadir). Both the SAR radar altimeter (SRAL) and OLCI are collocated but OLCI measurements are only available during periods of solar illumination. For example, Sentinel-3A SRAL measurements over the CDN1 transponder Cal/Val site are available at 20:00 UTC but no OLCI images are captured at this time of day (actually night).

On the other hand, simultaneous measurements of Sentinel-3B SRAL and OLCI instruments are made over the CDN1 Cal/Val site at 08:49:15 UTC every 27 days. Therefore, it is possible to directly compare the OLCI-derived *IWV* value at the 300m pixel, when the CDN1 site is observed, against the one GNSS-derived by the ground operating GNSS stations (Figure 13).

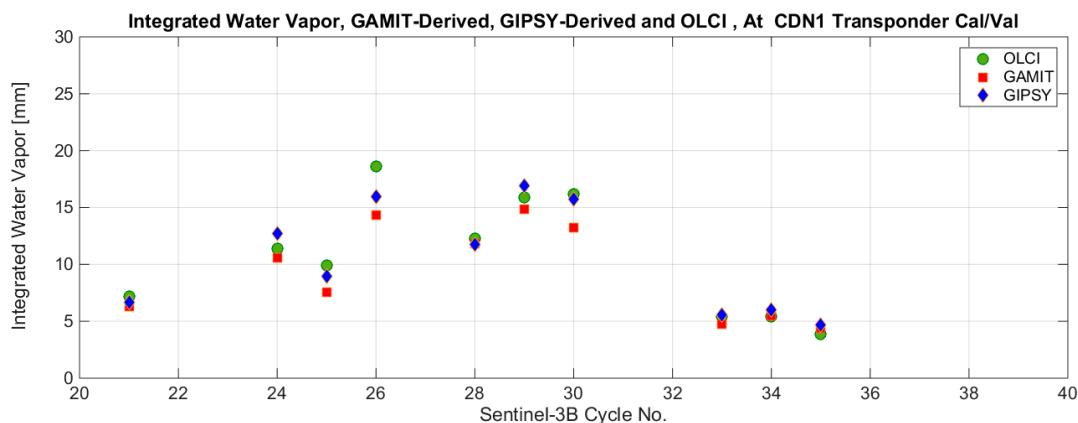


Figure 13. Comparison of the Integrated Water Vapor as measured by the Ocean Land Color Instrument (OLCI) instrument onboard Sentinel-3B, and estimated through GAMIT and GIPSY GNSS processing. The comparison takes place at the exact time of Sentinel-3B transponder calibrations at the CDN1 Cal/Val site and uses GNSS observations from the CDN0 station.

In Figure 13, this comparison is made for the CDN0 GNSS station using three independent techniques: relative differential, precise point positioning and OLCI imagery. In GAMIT, the *IWV* is computed as a secondary product in the GNSS processing. In GIPSY, the *IWV* value has been estimated using Equation (1). In this present analysis, only cloud-free conditions are considered in this OLCI investigation when a Sentinel-3B transponder calibration takes place. The comparison, as shown in Figure 3, starts after the Sentinel-3B satellite reached its nominal orbit.

It seems that, at the moment, there are four different techniques for determining the wet troposphere delays during transponder calibrations of the CDN1 Cal/Val site in West Crete. As more observations are accumulated, more reliable results will be reported.

3.3.2. FRM Uncertainty Estimation for Transponder Calibration

Several attempts have been made in [14,24] to estimate the uncertainty of the results in transponder calibration. Every time, a new and better estimate for some uncertainty constituents is presented as different elements of the uncertainty budget are improved. In fact, a primary application of a good uncertainty budget is to highlight the largest source of uncertainty in a measurement system, and then target that aspect for further improvement. In this manner, effort is given to the areas that will deliver the maximum improvement in performance, finally converging to a reliable measure of the uncertainty for transponder calibrations. In the same vein, Table 5 updates previous estimations for the uncertainty of the transponder calibration at the CDN1 transponder Cal/Val site.

Table 5. Uncertainty budget for the transponder calibration. The final standardized uncertainty (at 68% confidence level), described as Root-Sum-Square value, has been computed as:

$$FRM_{TRP}(Uncertainty) = \pm 34.46 \text{ mm} = \sqrt{(0.13)^2 + (3.50)^2 + (2.00)^2 + \dots + (17.32)^2 + (0.17)^2 + (11.55)^2}.$$

Error Constituent	Type	Uncertainty Estimate	Standard Uncertainty (Confidence 68%)
GNSS Height ¹	A	0.13 mm	±0.13 mm
GNSS Receiver ²	B	6.00 mm	±3.50 mm
GNSS Antenna Reference Point ¹	B	2.00 mm	±2.00 mm
Measured Range ²	B	3.00 mm	±1.73 mm
Transponder Internal Delay ¹	B	30.00 mm	±15.00 mm
Dry Tropospheric Delay ²	B	2.00 mm	±1.15 mm
Wet Tropospheric Delay ²	B	14.00 mm	±8.08 mm
Ionospheric Delay ²	B	4.00 mm	±2.31 mm
Geophysical Corrections ²	B	20.00 mm	±11.55 mm
Satellite Orbit Height ²	B	30.00 mm	±17.32 mm
Pseudo-Doppler Correction ¹	B	2.00 mm	±2.00 mm
Leveling Instrument/Method ¹	B	1.00 mm	±1.00 mm
Transponder Leveling ¹	A	0.50 mm	±0.16 mm
Processing and Approximations ²	B	30.00 mm	±17.32 mm
Orbit Interpolations ²	B	0.30 mm	±0.17 mm
Unaccounted effects ²	B	20.00 mm	±11.55 mm
Root-Sum-Squared Uncertainty			±34.46 mm

¹ Assuming that residuals are random and normally distributed, with no autocorrelation. ² Assuming that constituent uncertainty follows a uniform distribution.

In this Section, the uncertainty of the sea-surface and transponder calibration and for the procedures followed at the PFAC has been derived, following the FRM4ALT standards.

4. PFAC Calibration Results

This section presents the bias and uncertainty of the radar altimeters in Sentinel-3A, Sentinel-3B and Jason-3. First, absolute Cal/Val results are determined for each pass of the altimeters using the sea-surface and/or the transponder techniques. Then, relative calibration is carried out for the tandem phase of Sentinel-3A and Sentinel-3B, followed by crossover analysis for Sentinel-3A/Jason-3.

4.1. Sentinel-3A

Three Sentinel-3A passes are calibrated at the PFAC (Figure 14): The ascending Pass No. 14 with sea-surface and transponder calibration at the Gavdos and the CDN1 Cal/Val sites, respectively, the descending Pass No. 335 also using the Gavdos Cal/Val site, and the descending Pass No. 278 with the CRS1 Cal/Val site.

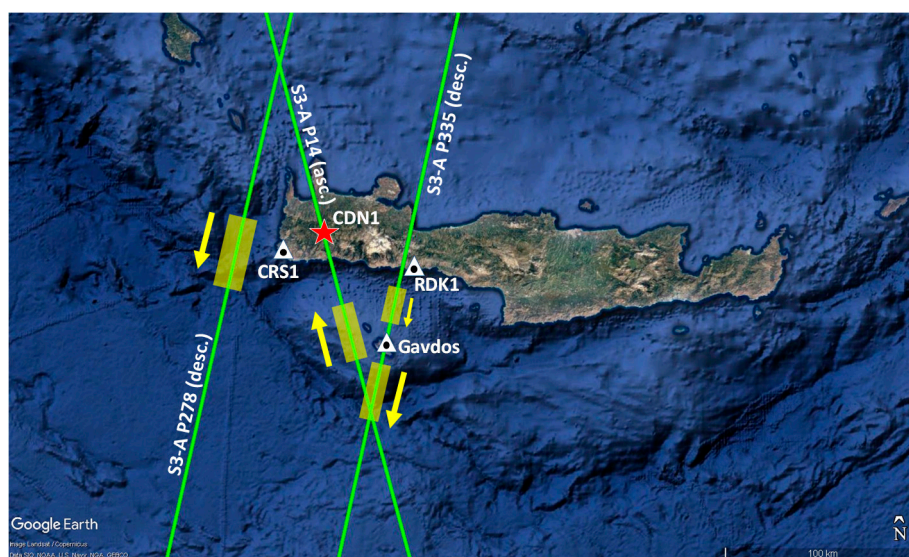


Figure 14. The Sentinel-3A sea-surface calibration regions for its Pass No. 14, No. 278 and No. 335 over the PFAC Cal/Val facility in west Crete, Greece. Sea-surface calibration is carried out at three different sea regions based upon the Gavdos, CRS1 and RDK1 Cal/Val sites. The CDN1 transponder Cal/Val site is also illustrated with a red star.

In Sections 3.1 and 3.2, the calibration processing of the in-situ ground measurements and models has been described. Satellite measurements also require some kind of rectification, as the altimeter and radiometer's observations are contaminated by the land mass of Gavdos and Crete. Regions with valid satellite measurements have to be identified and selected as calibrating regions for comparison with in-situ Cal/Val measurements. This process is carried out for each satellite's pass. Using the latest processing baseline for Sentinel-3A (version 2.61) that is common for all of its cycles, three sea-calibrating regions have been defined at the PFAC, as illustrated in Figure 14.

For a successful transponder calibration, the satellite altimeter generally needs to operate in “open-loop” mode. This is necessary to adjust its range gate to operate over the transponder's elevation and collect range measurements. The “open-loop” mode relies upon high-resolution Digital Elevation Models (DEM) stored in the altimeter or additionally with a direct commanding as in the Sentinel-6 case that additionally allows the fixing of the instrument gain given the transponder characteristics. Using this a-priori knowledge, the altimeter adjusts its internal receive window appropriately, and thus the signal amplified by the transponder can be received by the satellite altimeter. It is not the purpose of this work to explain the steps followed to process the waveforms for pulse-limited (e.g., Poseidon-3B in Jason-3) and delay-Doppler altimeters (i.e., SRAL/Sentinel-3A/B and Poseidon-4 Sentinel-6) to arrive at the value of range bias, as details can be found in [14,31].

Processing of Sentinel-3 waveforms is a complex procedure applied to about 200 radar bursts (of which about 30–40 bursts contain a useful transponder response over 1.5 to 2 s integration time) each of which contains 64 Ku-band pulses. Examples of altimeter waveforms that include the transponder's echo have been presented in Figure 2. The required parameters for transponder calibrations are obtained through Sentinel-3 telemetry and satellite calibration products [14].

4.1.1. Sentinel-3A Pass No. 14 Cal/Val Results

The ascending Sentinel-3A Pass No. 14 approaches the Gavdos island from the south. Calibration over sea surface is carried out using the Gavdos Cal/Val facility. About 9 s later, on its ascending pass, the satellite reaches the CDN1 transponder Cal/Val site where it is also calibrated (Figure 15). The bias in sea-surface height and range for Sentinel-3A along its Pass No. 14 are given in Figure 16 for all available passes at the time of writing.

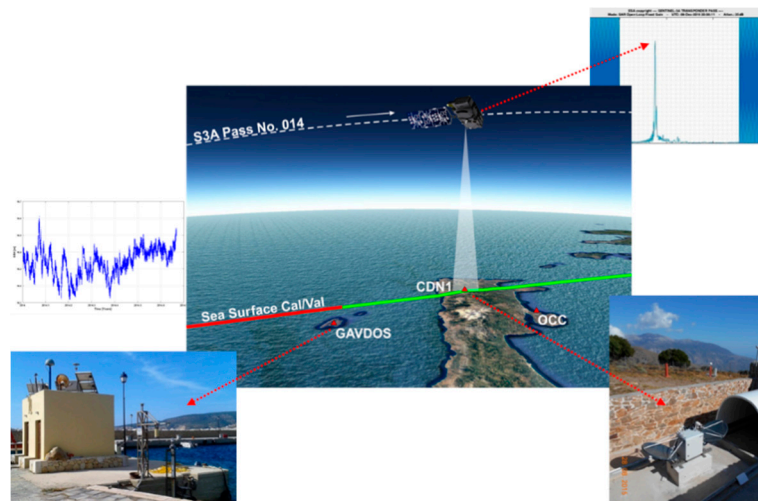


Figure 15. The Sentinel-3A Pass No. 14 is calibrated using both sea-surface and transponder calibration techniques at the Gavdos and CDN1 Cal/Val facilities, respectively.

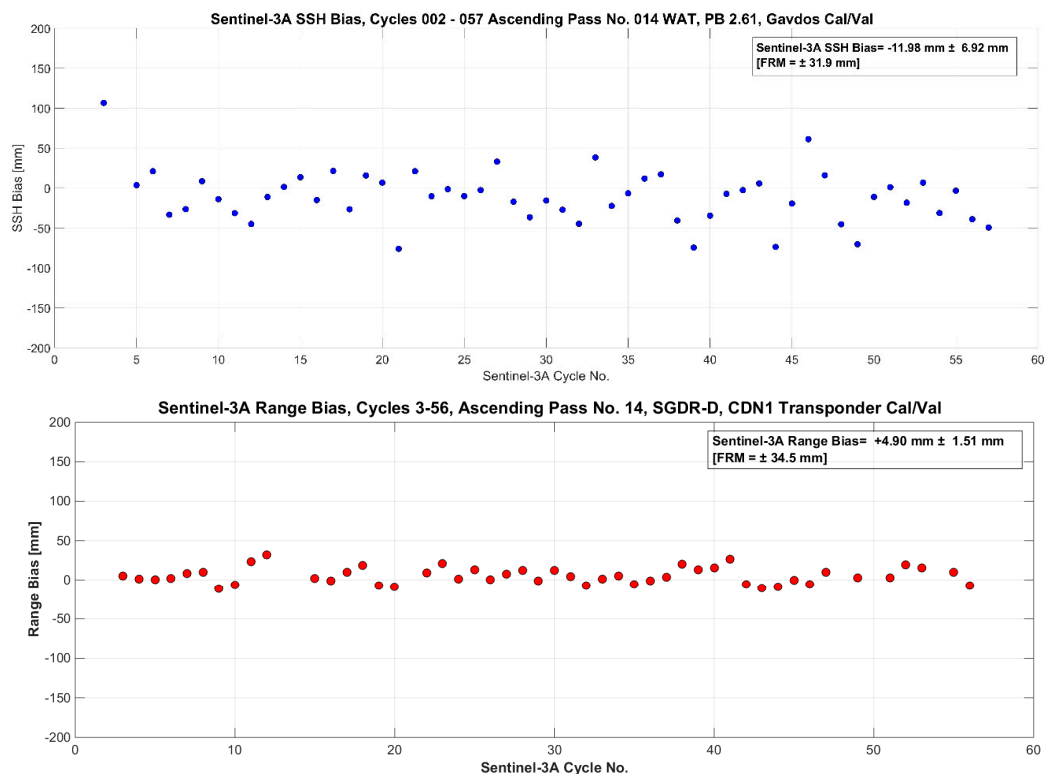


Figure 16. The latest calibration results for the ascending Pass No. 14 of Sentinel-3A using the sea-surface (upper) and transponder (lower) calibrations.

The sea-surface bias for Sentinel-3A Pass No. 14 is calculated as -11.98 mm , whereas the range bias with the transponder is determined as $+4.90 \text{ mm}$. These results indicate that the altimeter measures larger ranges than the “ground reference” by $+4.90 \text{ mm}$ with the present settings. The negative value of -11.98 mm in the SSH bias seems to support both Cal/Val results. The absolute difference between the two Cal/Val results is less than 1 cm , whereas the FRM uncertainty of each independent technique is of the order of $\pm 3 \text{ cm}$.

4.1.2. Sentinel-3A Pass No. 278 and No. 335 Cal/Val Results

Two sea-surface Cal/Val sites support the calibration of the descending Pass No.335 of Sentinel-3A (Figure 17). As the satellite descends, it meets first RDK1 Cal/Val where it is calibrated, and then about 6 s later it is again calibrated with the other Cal/Val site of Gavdos. The results obtained by these two Cal/Val sites agree at the sub-centimeter level. At this stage, the RDK1 Cal/Val results present somewhat larger dispersion compared to Gavdos Cal/Val. Larger scattering for the RDK1 Cal/Val may be caused by the employed calibrating region, covering a 35 km stretch (1000 km depth) of ocean water between Crete and Gavdos. That water stretch is shorter in length than that of the Gavdos south calibrating region (with 3000 m depth), and also fewer uncontaminated by land values are available for the satellite calibration (mountains of 2500 m height in the north of RDK1). Several updates and improvements of the marine geoid and the mean dynamic topography models in support of the RDK1 Cal/Val are currently ongoing.

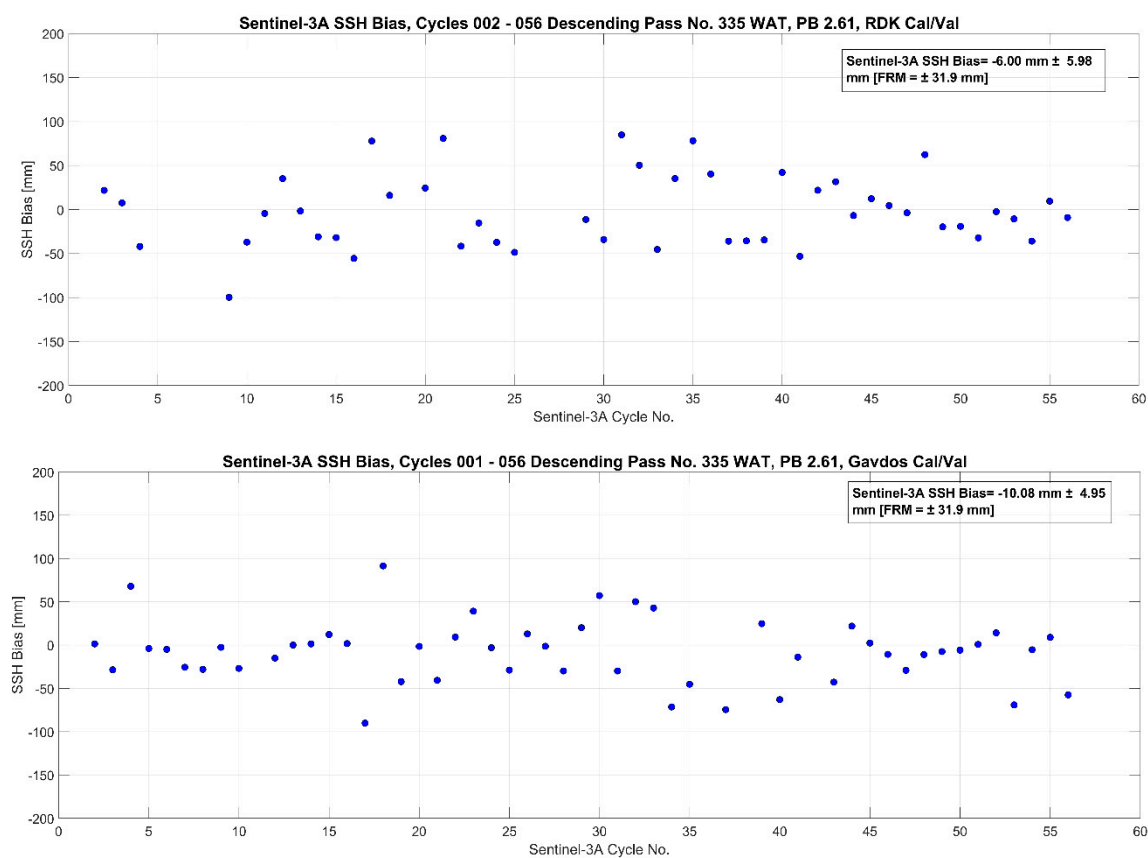


Figure 17. The latest calibration results for the descending Pass No. 335 of Sentinel-3A using the sea-surface calibration site located south of Crete site of RDK1 (upper) and the Gavdos Cal/Val sites (lower).

In the southwest tip of Crete, the CRS1 Cal/Val site provides support for the sea-surface calibration of the descending pass No. 278 of Sentinel-3A. Figure 18 presents the latest results for the Sentinel-3A. The estimated value for the bias in the sea-surface heights is found to be -3.68 mm based on this CRS1 Cal/Val site.

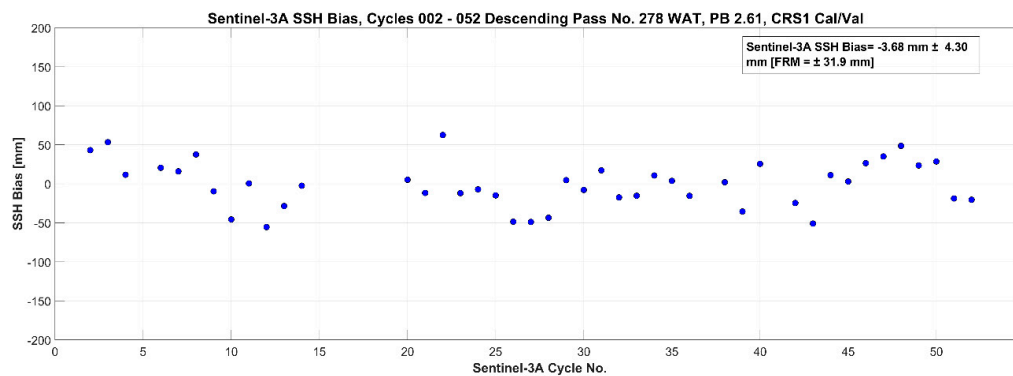


Figure 18. The latest calibration results for the descending Pass No. 278 of Sentinel-3A using the calibration methodology at the CRS1 Cal/Val site.

In summary, the bias in sea-surface height for Sentinel-3A has been determined to be on average -8.04 mm (± 5.5 mm, ± 32 mm FRM uncertainty) along its descending pass No. 335 based on Gavdos and RDK1 Cal/Val sites, while it is found to be -3.68 mm (± 4 mm, ± 32 mm FRM uncertainty) along another descending Pass of No. 278 and using the other CRS1 Cal/Val site. It appears that the bias of Sentinel-3A in sea-surface height, as monitored at the PFAC:

- Displays a negative sign for all these calibrating passes;
- Shows an average bias of -6.82 mm (± 32 mm FRM uncertainty) based on all three Cal/Val sites with descending orbits;
- Has no pass directional error in SSH bias as there is not significant trend at all between ascending and descending passes (-11.98 mm for Pass No. 14 and -8.04 mm for Pass No. 335).

4.2. Sentinel-3B Cal/Val

Three Sentinel-3B passes are calibrated at the PFAC. Calibration over sea surface is performed for the ascending Passes No. 14 and No. 71 at the CRS1 and RDK1 Cal/Val sites, respectively, using the latest processing baseline for Sentinel-3B (PB 1.33). The implemented calibration regions for Sentinel-3B are shown in Figure 19. The results refer to the Operational Phase of Sentinel-3B, which is when the satellite has been on its nominal orbit. Calibration results obtained during the Sentinel-3B Tandem Phase are given separately in Section 4.3.

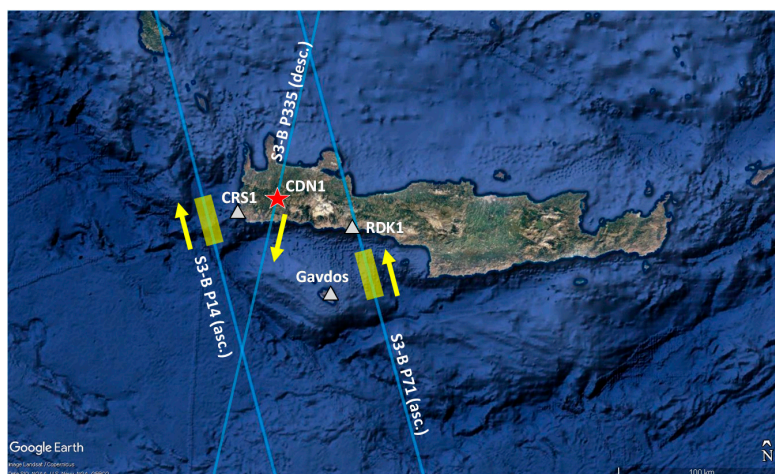


Figure 19. The Sentinel-3B calibrating regions over sea surface for its Pass No. 14, No. 71 and No. 335 in west Crete, Greece. Sea-surface calibration is carried out relying upon the CRS1 and RDK1 Cal/Val sites. The CDN1 transponder Cal/Val site has been used for the calibration of Sentinel-3B pass No. 335 (descending).

4.2.1. Sentinel-3B Transponder Cal/Val Results

The range bias of Sentinel-3B has regularly been determined at the CDN1 Cal/Val using its descending Pass No. 335, and continuously after Cycle No. 21 (5-February-2019). Figure 20 presents the results of this transponder calibration, covering its nominal satellite orbit.

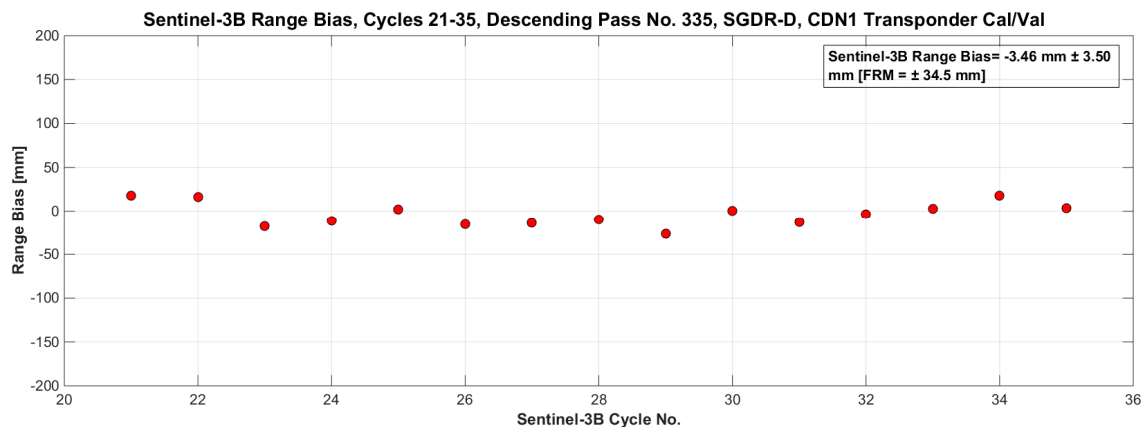


Figure 20. The latest calibration results of Sentinel-3B using its descending Pass No. 335 at the CDN1 transponder Cal/Val site.

The range bias of Sentinel-3B is calculated to be $B(S3B) = -3.46 \text{ mm} (\pm 3.50 \text{ mm}, \pm 35 \text{ mm FRM uncertainty})$. This value displays an opposite sign with respect to the previous Cal/Val results of Sentinel-3A (Section 4.1.1, $B(S3A) = +4.90 \text{ mm}$). In both satellites, the absolute value of their range bias appears to be about $\pm 5 \text{ mm}$: This means that Sentinel-3A and Sentinel-3B seem to measure altimetric distances of about 814 km as accurately as $\pm 5 \text{ mm}$ based on observations of this transponder.

4.2.2. Sentinel-3B Cal/Val Results Over Sea Surface

The CRS1 and RDK1 sea-surface Cal/Val sites provide ocean truth measurements for the calibration of the ascending Sentinel-3B Pass No. 14 and Pass No. 71, respectively. Figure 21 presents the calibration results of Sentinel-3B over sea surface as derived by these two Cal/Val sites.

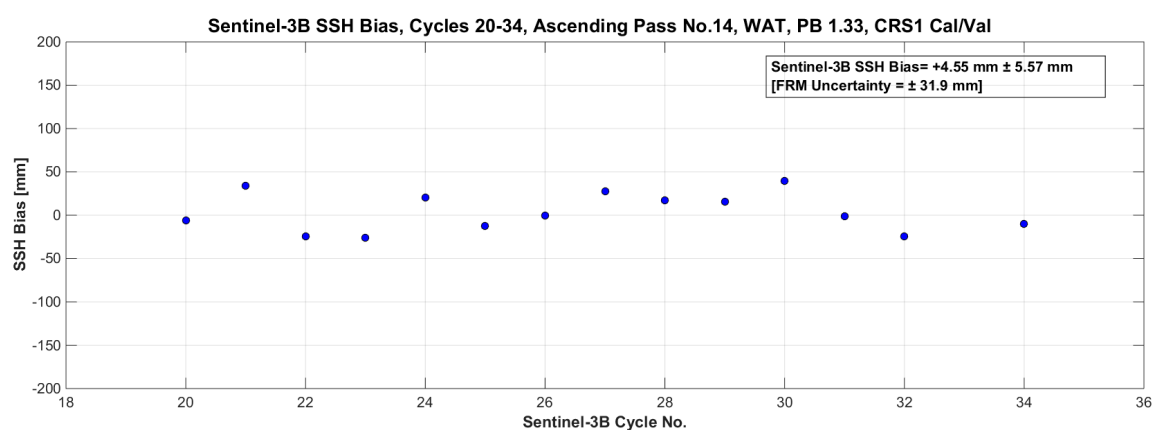


Figure 21. Cont.

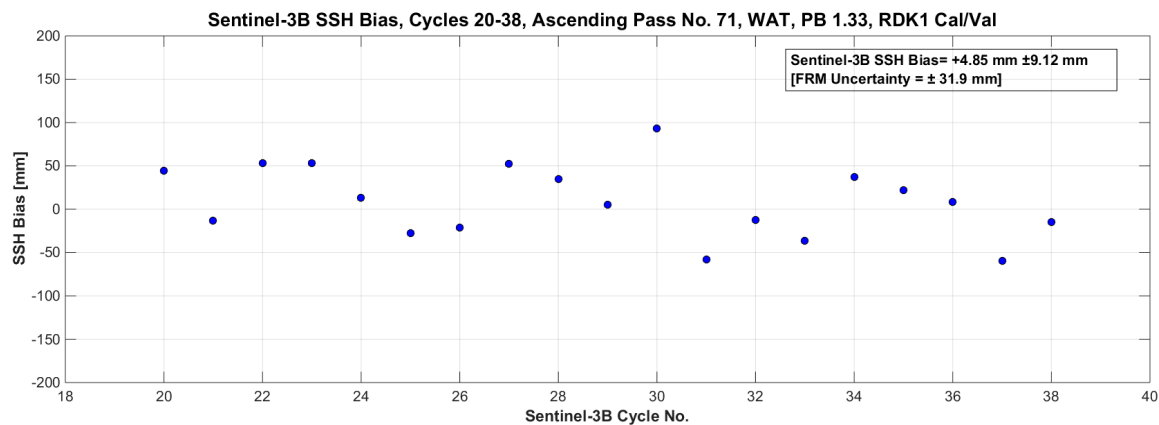


Figure 21. The latest calibration results of Sentinel-3B for its ascending Pass No. 14 (upper) and No. 71 (lower), using sea-surface calibration.

The bias of Sentinel-3B for the sea-surface height is +4.00 mm (± 7.50 mm, ± 32 mm FRM uncertainty) based on both ascending Pass No. 14 (B(S3B) = +4.55 mm, CRS1 Cal/Val) and Pass No. 71 (B(S3B) = +4.85 mm, RDK1 Cal/Val). As expected, the sign of the sea-surface height bias is opposite to the transponder range bias, while it appears that their magnitude agrees at the millimeter level.

4.3. Jason-3 Cal/Val Results

Jason-3 occupies a specific reference orbit for the multi-mission altimetry constellation. It flies on exactly the same ground-track as its predecessors TOPEX/Poseidon, Jason-1 and Jason-2, its repeat cycle is 10 days, and its measurements have provided accurate and consistent time-series for nearly three decades. In west Crete, the Gavdos Island is located under a crossover of Jason ground tracks of Pass No. 18 (descending) and Pass No. 109 (ascending) (Figure 22).

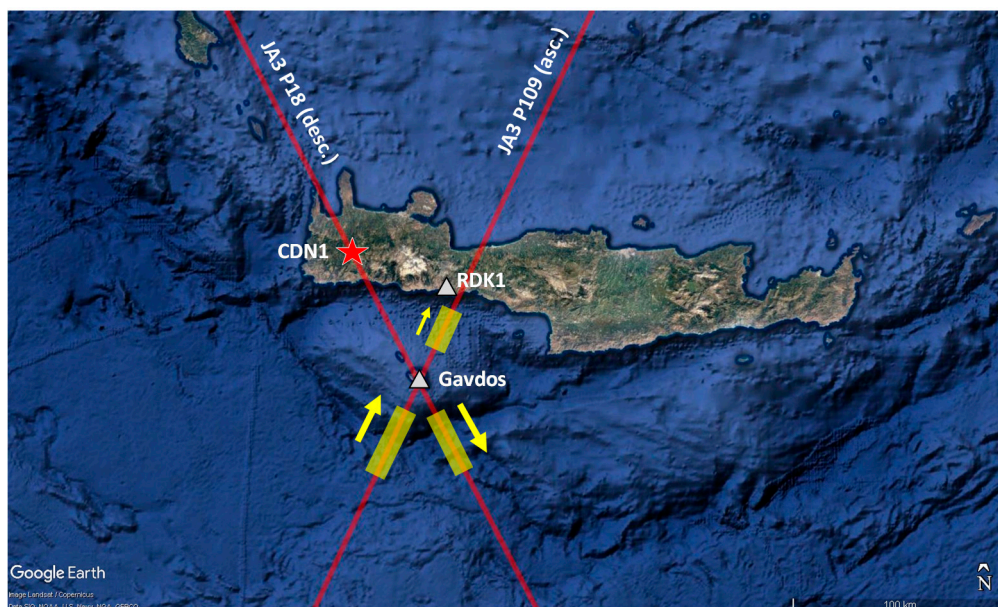


Figure 22. The sea-surface calibrating regions for Jason-3 along its Pass No. 109 and No. 018 over the PFAC Cal/Val facility. Sea-surface calibration is carried out at the Gavdos and at the RDK1 Cal/Val sites. The CDN1 transponder Cal/Val site has also been used for the calibration of Jason-3 Pass No. 18 (descending).

4.3.1. Jason-3 Cal/Val Results (No. 18)

Range as well as sea-surface calibrations are carried out for every cycle of Jason-3 Pass No. 18 using the CDN1 and Gavdos Cal/Val sites, respectively. First, the satellite passes over the CDN1 transponder Cal/Val site on the west Crete mountains and about 9 s later it reaches the Gavdos island in the south. Figure 23 presents the latest results in range and sea-surface calibration for Jason-3 over its descending Pass No. 18.

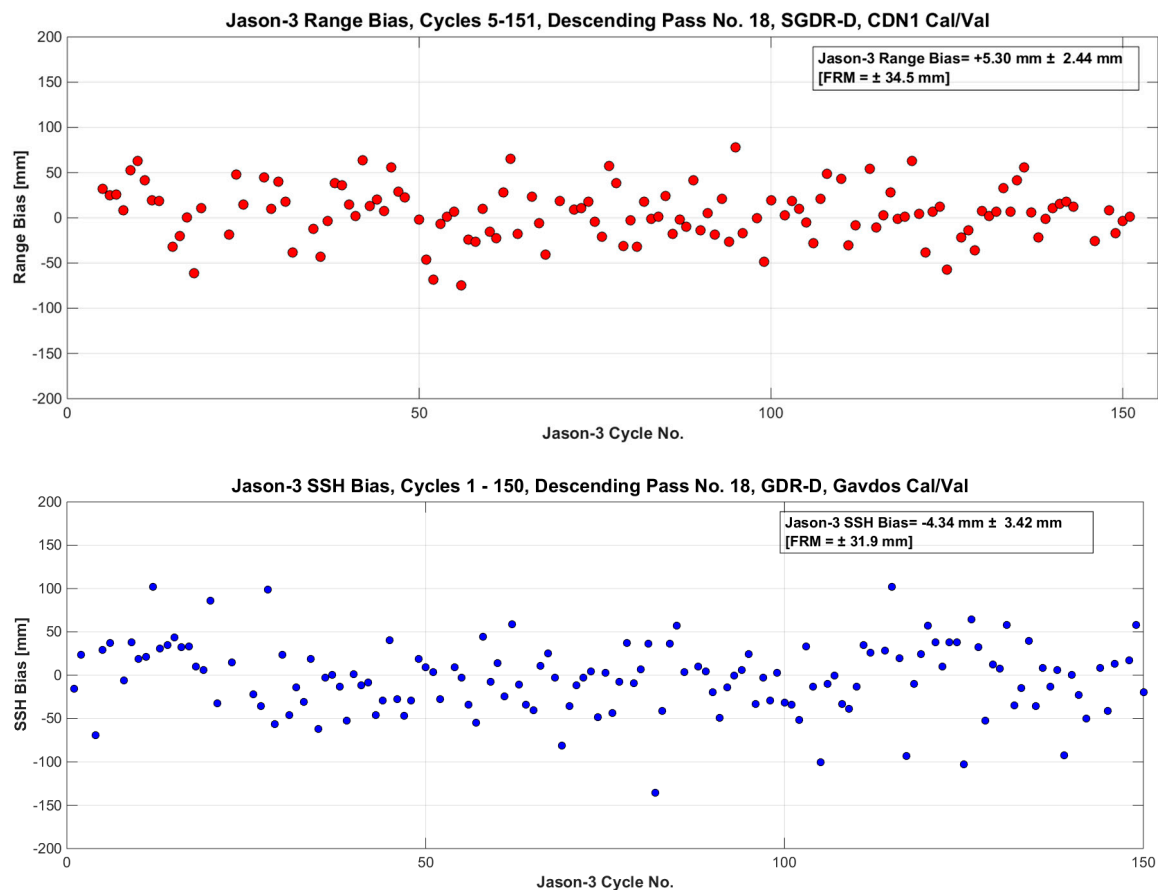


Figure 23. The latest calibration results for Jason-3 along its ascending pass No. 18 with transponder (upper) and sea-surface (lower) calibrations.

The sea-surface bias of Jason-3 is determined to be $B(JA3) = -4.34$ mm, whereas the transponder range bias is $B(JA3) = +5.30$ mm. As already described, the sign of the Jason-3 bias derived from the transponder and the sea-surface calibrations is opposite. Both calibrations result in the same absolute value of bias, thus supporting the reliability of the derived results.

4.3.2. Jason-3 Cal/Val Results (No. 109)

The ascending Pass No. 3 of Jason-3 has been calibrated over the sea surface using the Gavdos Cal/Val site. The latest calibration results for Jason-3, along the sea surface of Pass No. 109, with GDR-D data and for about 150 cycles, are given in Figure 24.

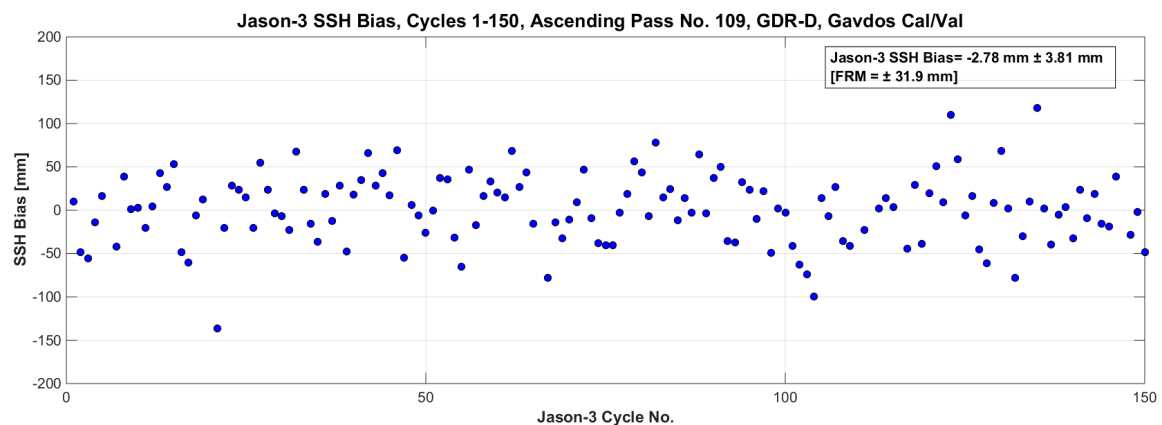


Figure 24. The Jason-3 calibration results for the sea-surface height, based on ascending pass No. 109 and using the Gavdos Cal/Val. The results cover cycles 1–150 with Geophysical Data Records-version D (GDR-D) data.

To recap, Sections 4.1 and 4.2 presented the sea-surface and transponder calibration results per altimeter mission and with respect to the Permanent Facility for Altimetry Calibration in west Crete, Greece. Table 6 summarizes the contribution of each PFAC Cal/Val site to the determination of the altimeter bias for Sentinel-3A, Sentinel-3B and Jason-3. Interpretation of these Cal/Val results per satellite follows at the end of Section 4.

Table 6. Latest calibration results for satellite altimetry missions as determined by four operational Cal/Val sites that comprise the Permanent Facility for Altimetry Calibration in west Crete, Greece. The Gavdos, CRS1 and RDK1 Cal/Val sites are used for sea-surface calibration, whereas the CDN1 is used for range transponder calibration.

Cal/Val Site/ Satellite	Sentinel-3A	Sentinel-3B	Jason-3
Gavdos	−11.98 mm (No. 14) −10.08 mm (No. 335)	−	−4.34 mm (No. 18) −2.78 mm (No. 109)
CRS1	−3.68 mm (No. 278)	+4.55 mm (No. 14)	
RDK1	−6.00 mm (No. 335)	+4.85 mm (No. 71)	
CDN1 Transponder	+4.90 mm (No. 14)	−3.46 mm (No. 335)	+5.30 mm (No. 18)

The Gavdos sea-surface Cal/Val site appears to produce consistent results per satellite altimeter. Two different passes in ascending and descending mode of Sentinel-3A and of Jason-3 are supported by the Gavdos Cal/Val facility. It seems that there is no significant difference for ascending and descending passes of Sentinel-3A and Jason-3. Moreover, the difference in bias results between transponder and sea-surface calibrations using the same orbit and with calibration taken place a few seconds apart, agree within ± 1 cm for Sentinel-3A (Pass No. 14, ascending) and for Jason-3 (Pass No. 18, descending). This setting clearly advocates the FRM requirements for having diverse, redundant and independent methodologies to assess performance of satellite altimeters.

4.4. Sentinel-3A -3B Cal/Val Results in Tandem Phase

Sentinel-3B was flying in tandem 30 s ahead of Sentinel-3A from 6-June-2018 to 17-October-2018 (Figure 25). Figure 26 presents the Cal/Val results for Sentinel-3A and Sentinel-3B during this tandem phase along sea surface Passes No. 14 (S3A), No. 278 and No. 335.

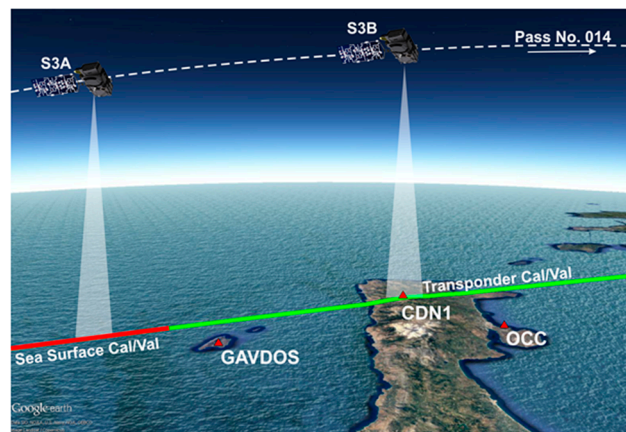


Figure 25. Sentinel-3A and -3B flying (not to scale) in tandem from June to October 2018 over west Crete, Greece and the transponder (CDN1) and sea-surface (Gavdos) permanent Cal/Val sites. Similar situations occurred for S3A and S3B for Pass No. 278 and No. 335 over the CRS1 and Gavdos sea-surface Cal/Val sites.

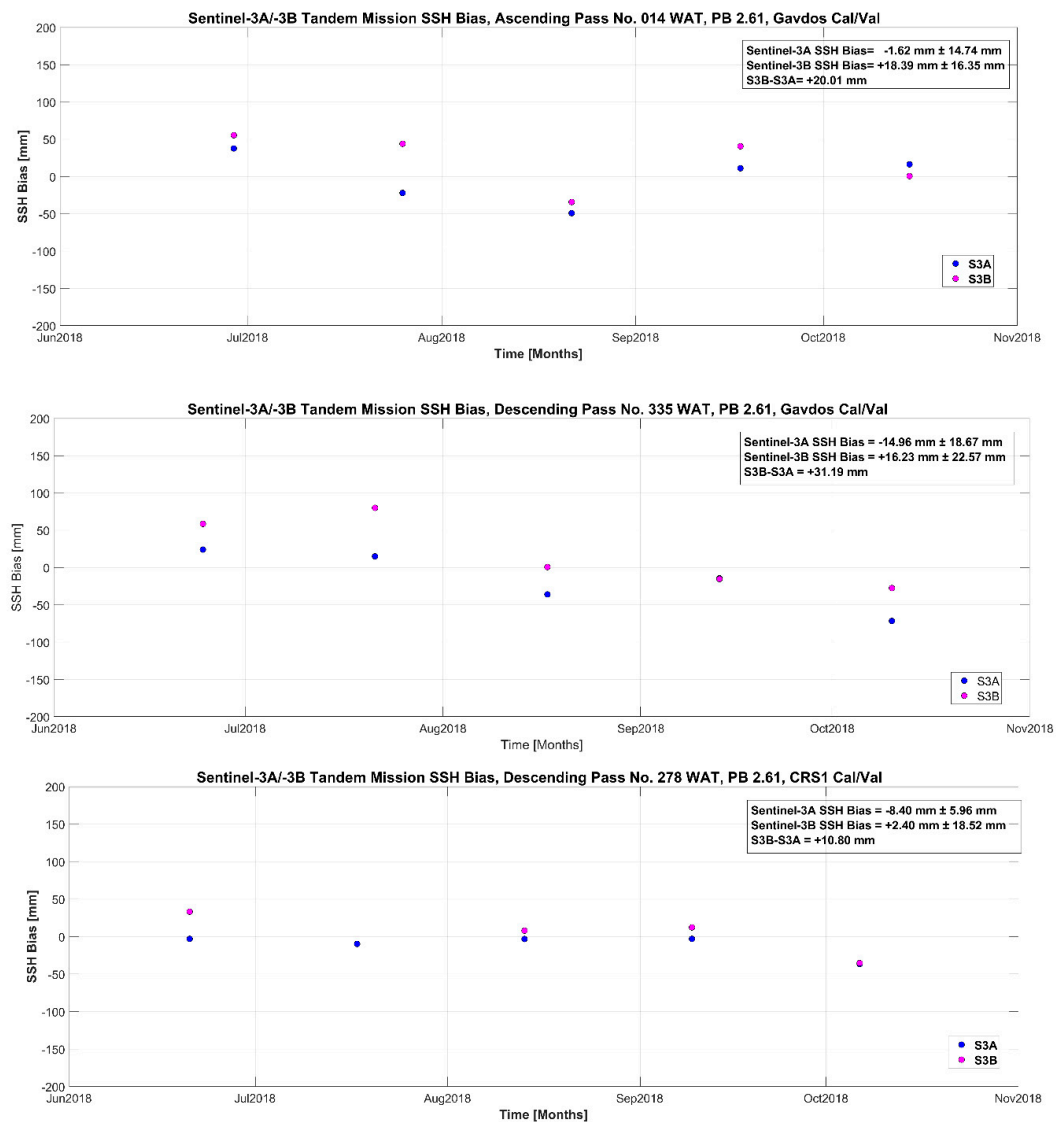


Figure 26. Sea-surface calibration results for Sentinel-3A and Sentinel-3B satellites during their tandem phase.

Over the sea surface and during tandem, the bias difference of Sentinel-3B with respect to Sentinel-3A is calculated to be +20.66 mm (average). This implies that Sentinel-3B seems to measure sea-surface height by +2 cm higher than Sentinel-3A, at least during their tandem phase. Nonetheless, this result is based only on very few cycles and thus cannot be statistically significant but only indicative.

During the tandem Sentinel-3A and Sentinel-3B phase, transponder calibrations were carried out at the CDN1 Cal/Val site (Figure 27). One of them was not successful, as Sentinel-3B's altimeter was operating in Low Resolution Mode. Here also, it can be seen that Sentinel-3A seems to measure a slightly shorter range than Sentinel-3B in that short transponder Cal/Val analysis.

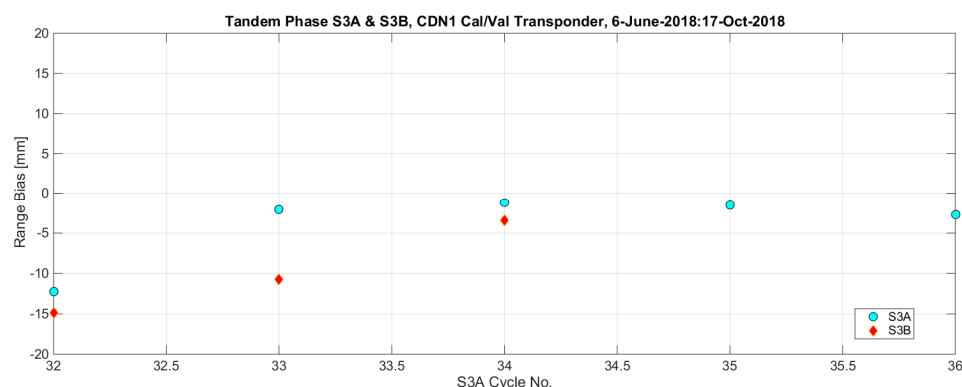


Figure 27. Transponder results for Sentinel-3A and Sentinel-3B satellites during their tandem phase. The bias results are given in mm to reveal slight differences between Sentinel-3A and Sentinel-3B.

Both results in sea surface and transponder analysis corroborate each other during the tandem phase of Sentinel-3A and Sentinel-3B. The analysis continues with crossover Cal/Val results.

4.5. Cal/Val Results at Crossovers

The groundtracks of the Sentinel-3A and Jason-3 intersect at a point (Lat = 34.63893946, Long = 23.98522449) about 20 km south of Gavdos island (Figure 3). To compare sea-surface heights observed by these two satellites at that crossover location with some confidence, their flyover had to be separated by no more than 2 days.

Between March 2016 and March 2020, this condition was fulfilled 19 times: 9 times the temporal separation of Sentinel-3A and Jason-3 was 1 day and 2 days (48-h) for the remaining cases. For each pair of altimeters, linear regression was carried out on orbital data to accurately determine the geodetic coordinates of their crossover location at sea. Then, the exact SSH value at the crossover location for each satellite altimeter was computed, taking into consideration the geoid models and the satellite direction in the region of crossover. Accordingly, 10 sampling points astride the crossover location have been used. These 20 altimeter observation points correspond to a distance of about 5 km along the satellite ground track.

Figure 28 presents the outcome of this crossover analysis. It can be seen that the dispersion of the relative bias is of the order of ± 4 cm but the average bias has been calculated to be +1.7 cm. This implies that Sentinel-3A measures the SSH +1.7 cm higher compared to Jason-3.

In addition, it seems that the uncertainty of this simplified and localized version of the multi-mission crossover analysis is similar to the FRM uncertainty (Tables 4 and 5) of the sea-surface and transponder calibrations. Note here that in crossover analysis no in-situ measurements were used.

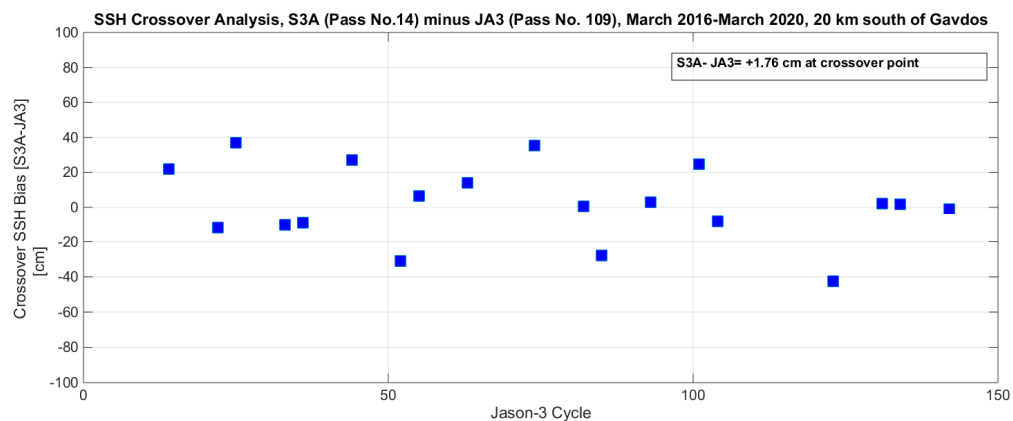


Figure 28. Relative sea surface height bias of Sentinel-3A and Jason-3 altimeters over their intersection point, 20 km south of Gavdos.

This section presented the latest calibration results for Sentinel-3A, Sentinel-3B and Jason-3 satellite altimeters as determined by diverse techniques at the PFAC. Table 7 provides a concise summary of these Cal/Val results.

The results of this investigation can be summarized as follows: (1) the bias in sea-surface height determination by the satellite altimeters is within their specification of ± 1.5 – 2.0 cm [17], (2) no significant drift in altimeters' performance has been monitored, (3) confidence on calibration results has been improved as diverse and independent Cal/Val techniques produce similar results, (4) the difference between sea-surface and transponder Cal/Val methodologies is within their FRM uncertainty, (5) Sentinel-3A measures sea-surface height higher than Jason-3, and (6) Sentinel-3B measures sea-surface height higher compared to Sentinel-3A.

Table 7. Absolute and relative calibration results for Sentinel-3A, Sentinel-3B and Jason-3 based on sea-surface, transponder techniques, as well as crossover analysis and S3A and S3B tandem phase analysis at the Permanent Facility for Altimetry Calibration. All values are in mm.

Sentinel-3A				Sentinel-3B			Jason-3		
Product Cycles Pass Range SSH(GVD,CRS1) SSH(RDK1) Mean SSH	PB2.61	PB2.61	PB2.61	Nominal Orbit PB2.61	PB2.61	PB2.61	GRD-D	GRD-D	
	2:57	2:52	1:56	20:34	20:38	21:35	1:150	1:150	
	No. 14	No. 278	No.335	No. 14	No.71	No.335	No. 18	No. 109	
	+5 mm	-	-	-	-	-4.51 mm	+5.60 mm	-	
	-12 mm	-4 mm	-10 mm	+4.55 mm	+4.85 mm	-	-4.34 mm	-2.78 mm	
		-6 mm							
-7.93 mm				+4.70 mm			-3.56 mm		
Tandem Phase									
Sentinel-3A				Sentinel-3B			S3B-S3A Offset		
Product		PB2.61		PB2.61					
Pass	P14	P278	P335	P14	P278	P335	P14	P278	P335
SSH	-1.62 mm	-8.40 mm	-14.96 mm	+18.39 mm	+2.40 mm	+16.23 mm	+20.01 mm	+10.80 mm	+31.19 mm
Mean								+20.66 mm	
Crossover Analysis									
Sentinel-3A Pass No. 14				Jason-3 Pass No. 109			S3A-Jason-3 Offset		
Cycles	1-56			1-149					
SSH							+17 mm ± 49 mm		

5. Discussion

This Section reviews calibration results of Section 4 in perspective of other Cal/Val works. It also elaborates upon future research and infrastructure upgrading, scheduled to take place at the PFAC. More specifically, the Sentinel-3 Mission Performance Center (S3MPC) has recently assessed the performance of Sentinel-3A and Sentinel-3B using independent processing of the CDN1 transponder data along with sea-surface calibration results using the Corsica, France permanent calibration facilities [32]. These S3MPC calibration results are compared against the range and sea-surface calibration results obtained at the PFAC. Furthermore, the on-going upgrading of the PFAC as a range and sigma-naught transponder facility is also presented.

5.1. Cross-Examination of Transponder Cal/Val Results

The S3MPC publishes the Sentinel-3 altimeter Cyclic Performance Reports. These reports assess the performance of the scientific instruments on-board Sentinel-3A and Sentinel-3B. They are available online [33]. The S3MPC report for the Cycle No. 56 of the SRAL altimeter of Sentinel-3A contains Sentinel-3A and Sentinel-3B range bias results using the CDN1 Cal/Val transponder. These results, as published by the S3MPC, have been determined independently to the PFAC methodology presented in Section 2. Figure 29 illustrates the range bias results as calculated by the S3MPC and the PFAC for Sentinel-3A Cycles 3–56 and Sentinel-3B Cycles 11–35 as of their launch dates: 16-Feb-2016 and 25-April-2018, respectively.

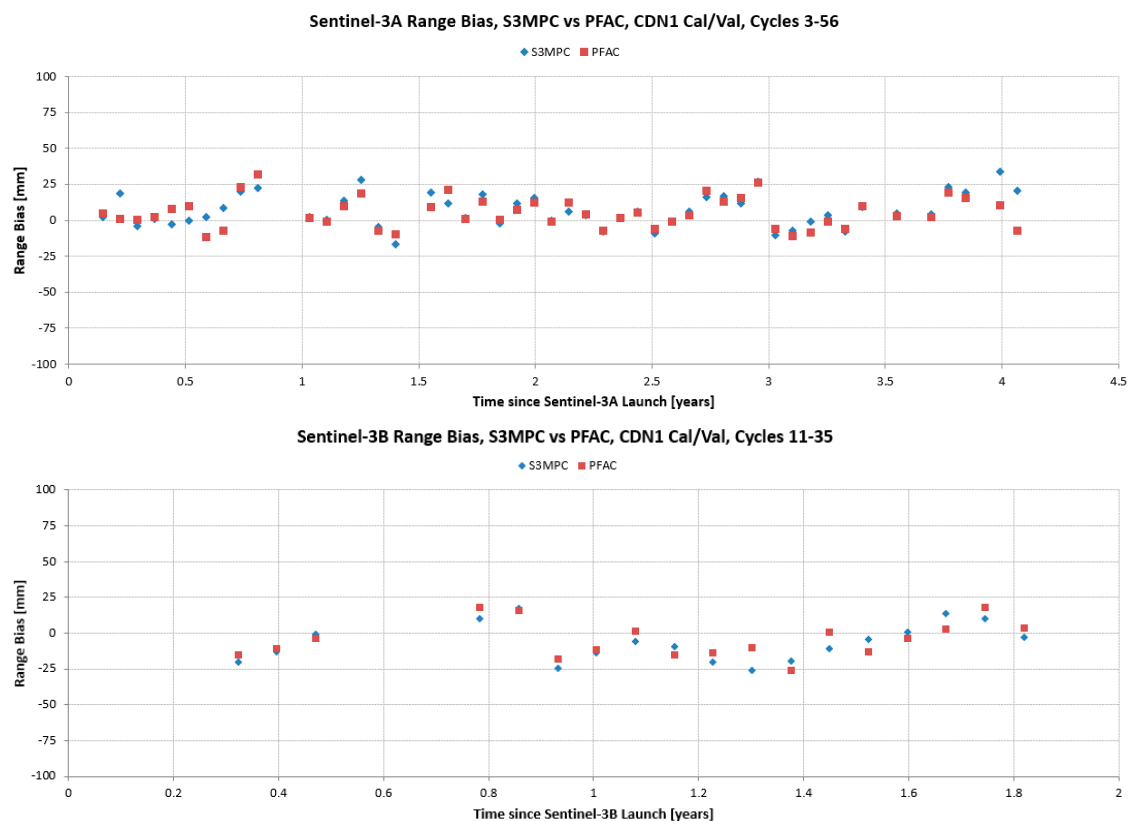


Figure 29. Absolute range calibration results for Sentinel-3A Pass No. 14 as determined by the Sentinel-3 Mission Performance Center and the PFAC based upon the transponder at the CDN1 Cal/Val site.

The range bias of Sentinel-3A and Sentinel-3B has been determined by the S3MPC to be +6.79 mm and −6.59 mm, respectively [29]. The same biases as presented under FRM methodology in this investigation (Table 7) are, respectively, +4.90 mm and −3.46 mm. Thus, there is an agreement of the two transponder processing techniques at the ± 2 mm level. This is within the expected uncertainty of the different and independent methods of data analysis used.

5.2. Cross-Examination of Sea-Surface Calibration Results

The Corsica, France calibration facility calculated the sea-surface height bias of Sentinel-3A and Sentinel-3B as +16 mm (S3A) and +19 mm (S3B), respectively [29]. The mean values of all passes calibrated at the PFAC have been (Table 7) −7.93 mm (S3A) and +4.70 mm (S3B), respectively. The deviation (S3MPC minus PFAC) between the calibration results is of the order of +2.5 cm for Sentinel-3A and +1.5 cm for Sentinel-3B. This discrepancy is within the reported FRM uncertainty of the PFAC sea-surface calibration results (± 34.5 mm, Table 5).

There are several other reasons that may explain the discrepancy between PFAC and S3MPC such as: (1) the S3MPC Cal/Val results are based on processing baseline No. 2.33 to 2.45 while the PFAC applied the latest PB.2.61, (2) Sentinel-3A Cal/Val results from the S3MPC refer to cycles 1 to 47, but this work is applied till cycle 56, (3) the S3MPC Cal/Val results for Sentinel-3B cover four cycles during its tandem phase with Sentinel-3A and not under its nominal orbit as determined for these PFAC results, and (4) in contrast to transponder Cal/Val where S3MPC used the same data (CDN1 transponder) as the PFAC, sea-surface calibration is carried out at different geographic locations, with different instrumentation and processing methodologies.

5.3. A Second Transponder in Gavdos

The European Space Agency FRM for the Sentinel-6 (FRM4S6) project is developing a prototype transponder to be installed and operated as part of the PFAC at Gavdos, called GVD1 Cal/Val, to ensure redundancy (FRM standard requirement) in transponder calibrations for Sentinel-6. This transponder is specifically responding to the need of Copernicus Sentinel-6. The second transponder is to calibrate not only the range but also the backscatter coefficient (sigma-naught, σ^0) of radar altimetry.

The backscatter coefficient (sigma-naught, σ^0) is a parameter that is useful for all Earth observing radars. It controls the efficiency of imaging radars when land deformations are observed at the mm level. It is used in radar scatterometers to determine wind speed and direction on the ocean surface and moisture determination in soil. It is also applied to radar altimeters to provide accurate measurements of the sea level, wave heights and wind speed over the ocean. Some ocean and meteorological models make use of satellite altimeter-derived wind speed and significant wave height observations. Indeed, the longest and most complete record of global ocean sea state is derived from satellite altimetry.

This transponder will be established at the GVD1 Cal/Val site under a triple crossover of Sentinel-6 (descending Pass No. 18, and ascending No. 109) and Sentinel-3A (descending Pass No.335) (Figure 30).



Figure 30. The location of the GVD1 transponder Cal/Val site in Gavdos island is under a crossover of the Sentinel-6 descending Pass No. 18, its ascending Pass No. 109 and the descending pass of Sentinel-3A Pass No. 335. The land of GVD1 is property of the Technical University of Crete. A permanent GNSS station has been operating there since 2004 (GVD0) whereas a Doppler Orbitography and Radiopositioning Integrated by Satellite (DORIS) beacon (GAVB) also operated for almost a decade (start 27-September-2003, end 27-March-2014).

The future research direction of the PFAC is to provide two alternative, independent techniques to perform range and sigma-naught calibration primarily for the upcoming Sentinel-6 [34]. Transponder and sea-surface Cal/Val is already carried at the PFAC, whereas the GVD1 transponder Cal/Val is to operate in late 2020 (Figure 31).

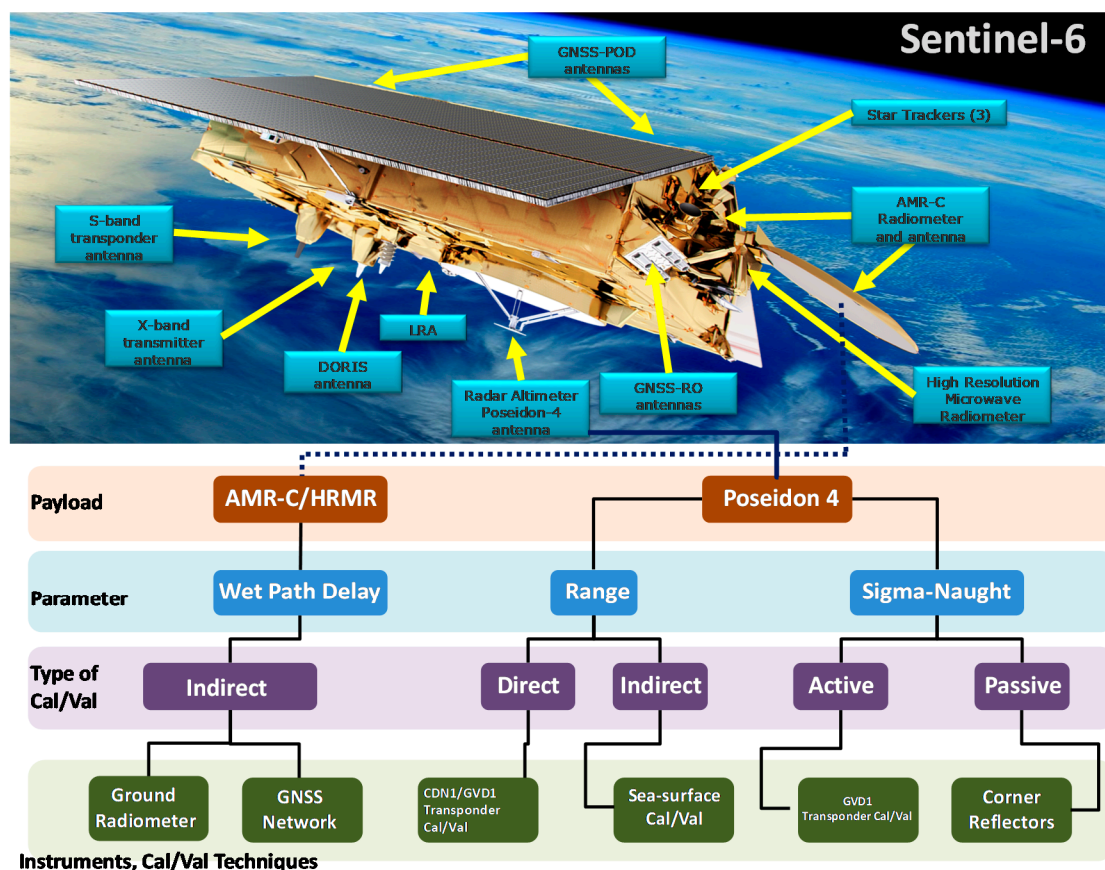


Figure 31. Flowchart of the way to calibrate Copernicus Sentinel-6 radar altimeter and its Advanced Microwave Radiometer-C (AMR-C) microwave radiometer at the Permanent Facility for Altimetry Calibration.

6. Conclusions

This work has provided a thorough assessment of the performance of Sentinel-3A, Sentinel-3B and Jason-3 satellite altimeters using the Permanent Facility for Altimetry Calibration of the ESA. Performance is monitored thorough land transponder and sea surface techniques at different locations and settings, as well as crossover analysis. Cal/Val results are accompanied by their uncertainty as calculated in the context of the new ESA strategy of Fiducial Reference Measurements.

The performance of all satellites appears to be within their design requirements, exhibiting altimetry biases of ± 1.5 – 2.0 cm. Figure 32 shows all results in a boxplot where all satellite altimeter biases, as presented in Table 7, are compared. It appears that transponder Cal/Val results in Sentinel-3A and Sentinel-3B are less dispersed (inter quantile range is smaller) than those in Jason-3. This may be attributed to the SAR mode of Sentinel-3 on one hand, but also to the implementation of Level-0 data in SAR calibration instead of Level-2 data carried out in Jason-3. Evaluation of the transponder and sea-surface calibration methodologies indicates that they both present an FRM uncertainty of the order of ± 3.0 – 3.5 cm.

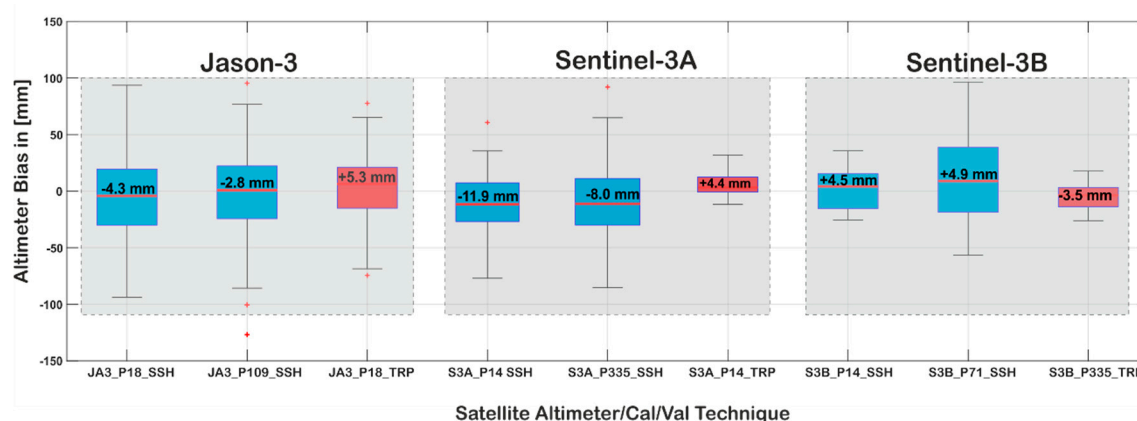


Figure 32. The Cal/Val results for Jason-3, Sentinel-3A and Sentinel-3B in box plots.

Calibration results derived by these two calibration techniques as well as relative calibration given by the crossover analysis all agree to within ± 1 cm. Sentinel-3 results are in agreement with results given by other Cal/Val groups, as previously described.

A major upgrade of the PFAC is currently under way. The target missions for this altimetry Cal/Val service would be primarily the Copernicus Sentinel-6 and Sentinel-3, while other international missions, such as Jason-3, HY-2, SWOT, CryoSat-2, etc., may benefit as well.

Author Contributions: Conceptualization, S.M., C.D. and C.M.; Methodology, S.M. and C.M.; Software, X.F., C.K., G.V.; Validation, X.F., I.N.T., and A.T.; Investigation, S.M., C.M., C.D., F.B., and P.F.; Resources, C.M., X.F., C.K., T.G. and A.T.; Data curation, X.F., C.K., and A.T.; Writing—original draft preparation, S.M. and A.T.; Writing—review and editing, S.M., C.D., A.T., R.C.; Visualization, X.F.; Supervision, S.M., P.F., and C.D.; Project administration, S.M., P.F., and C.D.; Funding acquisition, S.M. All authors have read and agreed to the published version of the manuscript.

Funding: This research was funded by European Union and the European Space Agency grant numbers [4000122240/17/I-BG and 4000129892/20/NL/FF/ab] and the APC was funded by Technical University of Crete.

Acknowledgments: We thank very much the three reviewers and the editor for their excellent and meticulous comments and observations made on this manuscript.

Conflicts of Interest: The authors declare no conflict of interest.

References

- Wilson, W.S.; Lindstrom, E.J.; Apel, J.R. Satellite Oceanography, History, and Introductory Concepts. In *Encyclopedia of Ocean Sciences*, 2nd ed.; Steele, J.H., Ed.; Academic Press: Salt Lake City, UT, USA, 2009; pp. 65–79, ISBN 9780123744739. [CrossRef]
- Ablain, M.; Meyssignac, B.; Zawadzki, L.; Jugier, R.; Ribes, A.; Spada, G.; Benveniste, J.; Cazenave, A.; Picot, N. Uncertainty in satellite estimates of global mean sea-level changes, trend and acceleration. *Earth Syst. Sci. Data* **2019**, *11*, 1189–1202. [CrossRef]
- Veng, T.; Andersen, O.B. Consolidating sea level acceleration estimates from satellite altimetry. *Adv. Space Res.* **2020**. [CrossRef]
- Nerem, R.S.; Beckley, B.D.; Fasullo, J.T.; Hamlington, B.D.; Masters, D.; Mitchum, G.T. Climate-change-driven accelerated sea-level rise detected in the altimeter era. *Proc. Natl. Acad. Sci. USA* **2018**, *115*, 2022–2025. [CrossRef] [PubMed]
- Oppenheimer, M.; Glanovic, B.C.; Hinkel, J.; van de Wal, R.; Magnan, A.K.; Abd-Elgawad, A.; Car, R.; Cifuentes-Jara, M.; DeConto, R.M.; Ghosh, T.; et al. Sea Level Rise and Implications for Low-lying Islands, Coasts and Communities. In *IPCC Special Report on Ocean and Cryosphere in a Changing Climate*; Portner, H.-O., Roberts, D.C., Masson-Delmotte, V., Zhai, P., Tignor, M., Poloczanska, E., Mintenbeck, K., Alegria, A., Nicolai, M., Okem, A., et al., Eds.; 2019; in press.
- IPCC. Available online: <https://www.ipcc.ch/srocc/chapter/chapter-4-sea-level-rise-and-implications-for-low-lying-islands-coasts-and-communities/> (accessed on 3 May 2020).

7. Hamlington, B.D.; Frederikse, T.; Nerem, R.S.; Fasullo, J.T.; Adhikari, S. Investigating the acceleration of regional sea level rise during the satellite altimeter era. *Geophys. Res. Lett.* **2020**, *4*, e2019GL086528. [CrossRef]
8. Kulp, S.A.; Strauss, B.H. New elevation data triple estimates on global vulnerability to sea-level rise and coastal flooding. *Nat. Commun.* **2019**, *10*, 4844. [CrossRef] [PubMed]
9. Mertikas, S.P.; Donlon, C.; Féménias, P.; Cullen, R.; Galanakis, D.; Frantzis, X.; Tripolitsiotis, A. *Fiducial Reference Measurements for Satellite Altimetry Calibration: The Constituents*; International Association of Geodesy Symposia; Springer: Cham, Switzerland, 2019; Volume 150, pp. 1–6. [CrossRef]
10. Donlon, C.J.; Minnett, P.J.; Wimmer, W. Chapter 5.2-Strategies for the Laboratory and Field Deployment of Ship-Borne Fiducial Reference Thermal Infrared Radiometers in Support of Satellite-Derived Sea Surface Temperature Climate Data Records. In *Experimental Methods in Sciences*; Elsevier: Waltham, MA, USA, 2015; Volume 47, pp. 557–603, ISBN 9780124170117. [CrossRef]
11. Mertikas, S.P.; Donlon, C.; Matsakis, D.; Mavrocordatos, C.; Altamimi, Z.; Kokolakis, C.; Tripolitsiotis, A. Fiducial reference systems for time and coordinates in satellite altimetry. *Adv. Space Res.* **2020**. [CrossRef]
12. Mertikas, S.; Donlon, C.; Féménias, P.; Mavrocordatos, C.; Galanakis, D.; Tripolitsiotis, A.; Frantzis, X.; Tziavos, I.N.; Vergos, G.; Andersen, O.B.; et al. Fifteen years of Cal/Val service to reference altimetry missions: Calibration of satellite altimetry at the Permanent Facilities in Gavdos and Crete, Greece. *Remote Sens.* **2018**, *10*, 1557. [CrossRef]
13. Mitchum, G. Monitoring the stability of satellite altimeters with tide gauges. *J. Atmos. Ocean. Technol.* **1998**, *15*, 721–730. [CrossRef]
14. Mertikas, S.P.; Donlon, C.; Féménias, P.; Mavrocordatos, C.; Galanakis, D.; Tripolitsiotis, A.; Frantzis, X.; Kokolakis, C.; Tziavos, I.N.; Vergos, G.; et al. Absolute calibration of the European Sentinel-3A surface topography mission over the permanent facility for altimetry calibration in west Crete, Greece. *Remote Sens.* **2018**, *10*, 1808. [CrossRef]
15. Adodo, F.I.; Remy, F.; Picard, G. Seasonal variations of the backscattering coefficient measured by radar altimeters over the Antarctic Ice Sheet. *Cryosphere* **2018**, *12*, 1767–1778. [CrossRef]
16. Pierdicca, N.; Bignami, C.; Roca, M.; Féménias, P.; Fascetti, M.; Mazzetta, M.; Loddo, C.N.; Martini, A.; Pinori, S. Transponder Calibration of the Envisat RA-2 altimeter Ku band sigma naught. *Adv. Space Res.* **2013**, *51*, 1478–1491. [CrossRef]
17. Giulicchi, I.; Tavernier, G.; Picot, N.; Cullen, R.; Scharroo, R.; Martin-Puig, C.; Desai, S.; Desjonquieres, J.D.; Leuliette, E.; Egido, A. *Sentinel-6/Jason-CS Cal/Val Concept*; JC-PL-ESA-MI-0500; European Space Research and Technology Centre: Noordwijk, The Netherlands, 2019; Available online: <https://cutt.ly/1yctabF> (accessed on 7 May 2020).
18. Egido, A.; Smith, W.H.F. Fully focused SAR Altimetry: Theory and Applications. *IEEE Trans. Geosci. Remote Sens.* **2017**, *55*, 392–406. [CrossRef]
19. Dettmering, D.; Schwatke, C. Multi-mission Cross-calibration of satellite altimeters. In *Fiducial Reference Measurements for Altimetry*; Mertikas, S., Pail, R., Eds.; International Association of Geodesy Symposia; Springer: Cham, Switzerland, 2019; Volume 150, pp. 49–54. [CrossRef]
20. Bosch, W.; Dettmering, D.; Schwatke, C. Multi-mission cross-calibration of satellite altimeters: Constructing a long-term data record for global and regional sea level change studies. *Remote Sens.* **2014**, *6*, 2255–2281. [CrossRef]
21. Romanazzo, M.; Jauregui, L.; Morales, J.; Emanuelli, P.P. Tandem operations preparation for Sentinel-3 A/B: Paving the way for C/D models. In Proceedings of the 15th International Conference on Space Operations, Marseille, France, 28 May–1 June 2018; American Institute of Aeronautics and Astronautics: Reston, VA, USA, 2018. [CrossRef]
22. Donlon, C.J.; O'Carroll, A.; Smith, D.; Scharroo, R.; Bourg, L.; Kwiatowska, E.; Merchant, C.; Sathyendranath, S.; Labrue, S.; Larnicol, G. *Scientific Justification for a Tandem Mission Between Sentinel-3A and Sentinel-3B during the E1 Commissioning Phase*; European Space Agency Technical Note EOP-SM/3057/CD-cd; V4.2; European Space Agency: Noordwijk, The Netherlands, 2016.
23. Donlon, C.; Scharroo, R.; Willis, J.; Leuliette, E.; Bonnefond, P.; Picot, N.; Schrama, E.; Brown, S. *Sentinel-6A/B/Jason-3 Tandem Phase Configurations*; ESA TN JC-TN-ESA-MI-0876 V2.0; European Space Agency: Noordwijk, The Netherlands, 2019.
24. Mertikas, S.P.; Donlon, C.; Vuilleumier, P.; Cullen, R.; Féménias, P.; Tripolitsiotis, A. An action plan towards fiducial reference measurements for altimetry. *Remote Sens.* **2019**, *11*, 1993. [CrossRef]

25. Herring, T.A.; King, R.W.; McClusky, S.C. *GAMIT reference Manual: GPS Analysis at MIT, Release 10.4*; Massachusetts Institute of Technology: Cambridge, MA, USA, 2010.
26. Desai, S.; Kuang, D.; Bertiger, W. *GIPSY/OASIS (GIPSY) Overview and under the Hood*; California Institute of Technology: Pasadena, CA, USA, 2014. Available online: ftp://ehzftp.wr.usgs.gov/svarc/GIPSY_pdfs/GIPSY_Overview.pdf (accessed on 7 May 2020).
27. Mígues, B.M.; Testut, L.; Wöppelmann, G. The Van de Casteele Test Revisited: An efficient approach to tide gauge error characterization. *J. Atmos. Ocean. Technol.* **2008**, *25*, 1238–1244. [[CrossRef](#)]
28. IOC. Manual on sea level measurement and interpretation, v. IV: An update to 2006. In *Intergovernmental Oceanographic Commission of UNESCO*; United Nations Educational, Scientific and Cultural Organization: Paris, France, 2006; p. 78.
29. Mertikas, S.P.; Daskalakis, A.; Tziavos, I.N.; Andersen, O.B.; Vergos, G.; Tripolitsiotis, A.; Zervakis, V.; Frantzis, X.; Partsinevelos, P. Altimetry, bathymetry and geoid variations at the Gavdos permanent Cal/Val facility. *Adv. Space Res.* **2012**, *51*, 1418–1437. [[CrossRef](#)]
30. BIPM. *International Vocabulary of Metrology-Basic and General Concepts and Associated Terms (VIM)*, 3rd ed.; JCGM/WG 2 Doc. N313; Bureau Int. des Poids et Mesures: Sevres, France, 2012.
31. Hausleitner, W.; Moser, F.; Desjonqueres, J.D.; Boy, F.; Picot, N.; Weingrill, J.; Mertikas, S.; Daskalakis, A. A new method of precise Jason-2 altimeter calibration using a microwave transponder. *Mar. Geod.* **2012**, *35* (Suppl. 1), 337–362. [[CrossRef](#)]
32. Quartly, G.D.; Nencioli, F.; Raynal, M.; Bonnefond, P.; Garcia, P.N.; Garcia-Mondéjar, A.; de la Cruz, A.F.; Crétaux, J.-F.; Taburet, N.; Frery, M.L.; et al. The roles of the S3MPC: Monitoring, validation and evolution of Sentinel-3 altimetry observations. *Remote Sens.* **2020**, *12*, 1763. [[CrossRef](#)]
33. Sentinel-3 Data Product Quality Reports. Available online: <https://sentinels.copernicus.eu/documents/247904/4069459/Sentinel-3-MPC-ISD-SRAL-Cyclic-Report-056-037.pdf> (accessed on 20 May 2020).
34. Scharroo, R.; Bonekamp, H.; Ponsard Ch Parisot, F.; Von Engeln, A.; Tahtadjiev MDe Vriendt, K.; Montagner, F. Jason continuity of services: Continuing the Jason altimeter data records as Copernicus Sentinel-6. *Ocean Sci.* **2016**, *12*, 471–479. [[CrossRef](#)]



© 2020 by the authors. Licensee MDPI, Basel, Switzerland. This article is an open access article distributed under the terms and conditions of the Creative Commons Attribution (CC BY) license (<http://creativecommons.org/licenses/by/4.0/>).